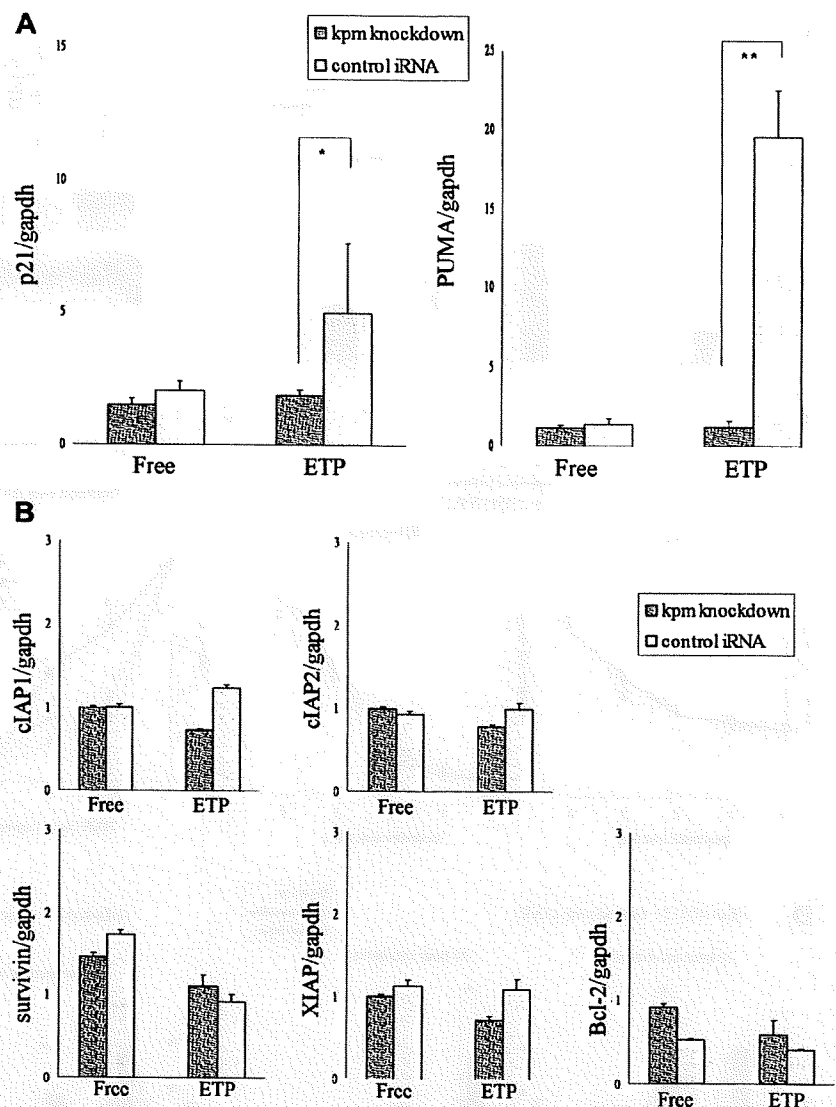


**Figure 3.** Induction of p21<sup>WAF1</sup> and PUMA but not the IAP family members or bcl-2 is repressed in Kpm/Lats2-knockdown KG-1a cells after treatment with DNA damage-inducing agents. Total mRNA was isolated from Kpm/Lats2-knockdown KG-1a or control cells treated with or without 0.03  $\mu$ g/mL ETP at day 0 and cultured for 3 days. mRNA expression levels of p21 and PUMA (A), and the IAP family members and bcl-2 (B), were measured by real-time PCR analysis using the specific primers described in Table 1. Data normalized to gapdh are shown as mean plus or minus SD in scale that the value for KG-1a wild-type cells without treatments is 1. Normalization to hprt gave similar results. The analyses were performed in triplicate independently twice, and representative data are shown (Student *t* test: \**P* < .05; \*\**P* < .005).



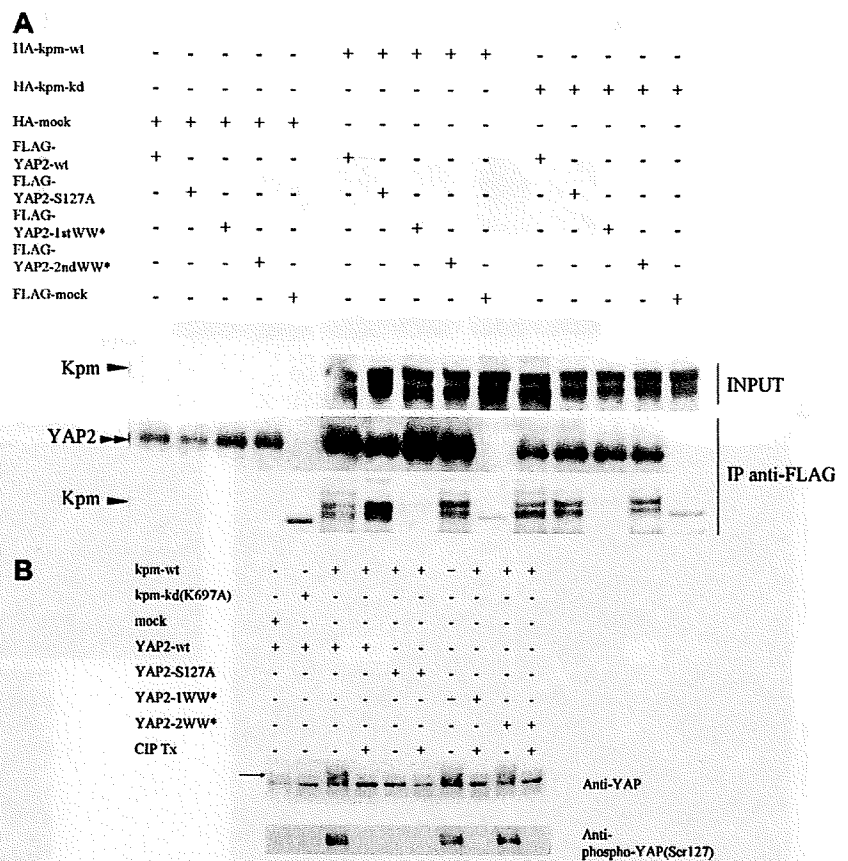
difference in the expression level of p73 mRNA after treatment with ETP between Kpm/Lats2-knockdown cells and control cells (Figure 4B). Similar results were obtained with microRNA-373-transduced KG-1a cells (Figure S5). Next, we evaluated the distribution of p73 protein by immunofluorescence microscopy because transcriptional activity of p73 depends on the accumulation of p73 in nucleus due to posttranscriptional modification.<sup>58</sup> p73 was scarcely detected in KG-1a cells with or without silencing of Kpm/Lats2 under normal conditions (data not shown) but was significantly induced in control KG-1a cells after treatment with ETP (Figure 4C). In contrast, p73 remained at very low levels in Kpm/Lats2-knockdown KG-1a cells (Figure 4C). Under higher magnification, we visualized more clearly that p73, which should accumulate in the nucleus, was hardly detected or only faintly represented in Kpm/Lats2-knockdown cells (Figure 4C). Moreover, we investigated the recruitment of p73 on the PUMA gene promoter after DNA-damage stress. ChIP assay clearly showed that p73 was recruited to the PUMA gene promoter in control cells but not in Kpm/Lats2-knockdown cells after DNA-damage stress (Figure 4D). In summary, our data suggest that Kpm/Lats2 contributes to the stability of p73 protein, which in turn leads to transcriptional induction of p21 and PUMA to finally trigger cell death after treatment with DNA damage-inducing reagents.

#### Kpm/Lats2 can associate with YAP2 via the first WW domain and induce its phosphorylation

We investigated whether Kpm/Lats2 could interact with and phosphorylate YAP as demonstrated in *Drosophila*. YAP has 2 major functional isoforms, YAP1 and YAP2, and we found that YAP2 was a dominant form expressed in hematopoietic lineage cells (Figure S2). Coimmunoprecipitation analyses indicated that Kpm/Lats2 interacted with YAP2 via its first WW domain (Figure 5A) and YAP1 via its only WW domain (Figure S5). In addition, coexpression of Kpm/Lats2 and YAP2 resulted in a mobility shift of YAP2. This mobility shift was abrogated by phosphatase treatment and was not caused by coexpression of the Kpm-kinase-dead form and YAP2. Therefore, this shift is indeed due to the phosphorylation of YAP protein (Figure 5B). It was unexpected, however, that this mobility shift occurred with the first WW domain mutant but not with the S127A mutant form of YAP2. Phosphorylation of YAP2 at serine 127 was further confirmed by Western blot using anti-phospho-YAP, which could recognize phosphorylated serine 127 of YAP2 specifically. In accordance with mobility shift assay, the phosphorylated YAP2 was clearly detected in coexpression of wild-type Kpm/Lats2 but barely detectable in coexpression of



**Figure 5.** Kpm/Lats2 can associate with YAP2 via its first WW domain and phosphorylate YAP2, but it requires not this association but kinase function of Kpm/Lats2 to stabilize p73. (A) Any one of HA-tagged Kpm-wild type (wt), Kpm-kinase dead (kd), or mock was cotransfected with any one of FLAG-tagged YAP2-wild type (wt), YAP2-S127A (mutant form S127 to A; S127 is Akt-phosphorylation site), YAP2-1WW\* (mutant form of first WW domain), YAP2-2WW\* (mutant form of second WW domain), or mock into 293T cells by the calcium phosphate method. Upper lanes represent Western blotting with anti-HA in cell lysates. Middle lanes and lower lanes represent Western blotting with anti-FLAG and anti-HA, respectively, in the immunoprecipitates by anti-FLAG. Three independent experiments were performed and representative data are shown. (B) The coimmunoprecipitate fraction by anti-FLAG from each lysate was treated with or without CIP and then analyzed by Western blotting with anti-YAP polyclonal antibody and anti-phospho-YAP (Ser127) polyclonal antibody. Arrow indicates mobility shift band of YAP2. Three independent experiments were performed and representative data are shown.



cells, and the protein levels of these molecules were estimated by Western blot. These transient coexpression experiments showed that the protein level of p73 was high in coexpression of wild-type YAP2 and wild-type Kpm/Lats2 but not the kinase-dead form or mock. High expression of p73 was observed not only in coexpression of the second WW domain mutant of YAP2 that was able to interact with Kpm/Lats2 but also in that of the first WW domain mutant of YAP2 that was unable to do that. On the other hand, the expression level of p73 was not increased in coexpression of the S127A mutant of YAP2 compared with mock. Furthermore, coexpression of wild-type Kpm/Lats2 but not the kinase-dead form augmented the protein level of YAP2 regardless of the presence of the first WW domain, and even wild-type Kpm/Lats2 did not affect the protein level of the S127A mutant of YAP2 (Figure 6). Similar results were obtained in the experiments of coexpression of Kpm/Lats2 and YAP1 (Figure S6). Considering that YAP is an important cofactor that associates with and stabilizes p73, the increase in p73 expression may be due to its stabilization by facilitated interaction with YAP2 mediated by its phosphorylation by Kpm/Lats2. Overall, these findings suggest that Kpm/Lats2 is involved in the stabilization of p73 by increasing the protein level of YAP2, which is dependent on the serine 127 of YAP2 and the kinase function of Kpm/Lats2.

## Discussion

*Drosophila* Warts/Lats is considered to be a tumor suppressor since its loss of function mutation results in overproliferation phenotype in mosaic animals.<sup>1,2</sup> The equivalent experiment has not been reproduced with Kpm/Lats2 in mammals because Kpm/Lats2 knockout mice are embryonically lethal.<sup>26,27</sup> Nevertheless, down-

regulation of Kpm/Lats2 has been described in a variety of human cancers.<sup>42,43,59</sup> Notably, low level of Kpm/Lats2 expression correlated with poor prognosis in ALL.<sup>43</sup> Therefore, we focused on the cellular changes caused by down-regulation of Kpm/Lats2 expression. The most intriguing finding was that silencing of Kpm/Lats2 in 2 types of leukemic cells resulted in increased resistance to DNA damage-inducing agents. The viability of Kpm/Lats2-knockdown KG-1a cells after treatment with ETP or DXR was consistently higher than that of wild-type or control cells. This tendency was also observed in Kpm/Lats2-knockdown ED-40515<sup>+</sup> cells. Based on the findings of Hippo pathway in *Drosophila*, we expected that a direct executor may be one of the IAP family members because IAPs are major inhibitor of caspases, but the mRNA expression levels of IAP family members were not altered in Kpm/Lats2-knockdown cells. To find out what molecules could directly cause such resistance, we used real-time PCR analysis to search for altered expression of several candidate genes related to cell-cycle arrest or apoptosis. Among the candidates we screened, induction of p21 and PUMA by treatment with ETP was markedly suppressed in Kpm/Lats2-knockdown cells compared with control shRNA-transduced cells that responded with high levels of these genes. p21 is a well-known CDK inhibitor that induces cell cycle arrest,<sup>60</sup> and PUMA is a final executor that localizes BAX onto mitochondrial membrane to trigger apoptosis.<sup>56</sup> Therefore, the suppressed induction of these genes in Kpm/Lats2-knockdown KG-1a cells seems to be compatible with their resistance to DNA damage-inducing agents.

Expression of both p21 and PUMA is induced by p53 and its family members. Since KG-1a cells<sup>53</sup> and ED-40515<sup>+</sup> cells are p53 null (Dr M. Matsuoka, Kyoto University, e-mail communication,

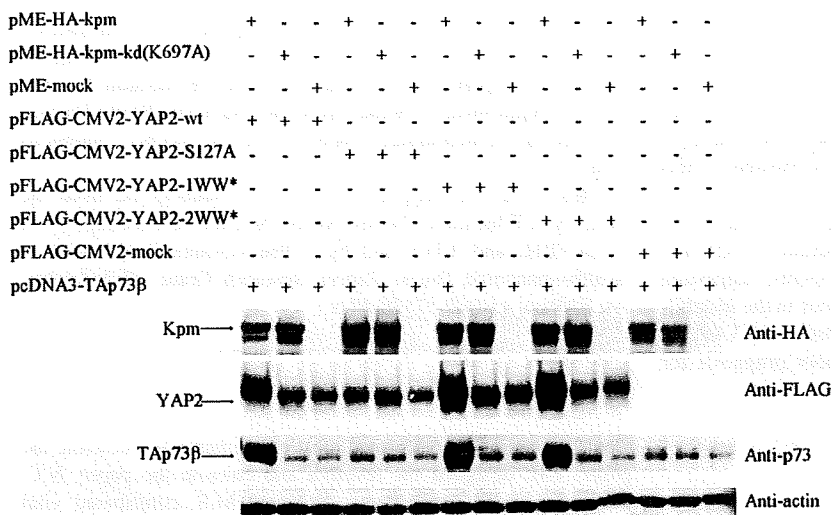


**Figure 6. The protein level of p73 is increased by coexpression of YAP2 and wild-type Kpm/Lats2.** Any one of HA-tagged Kpm-wild type (wt), Kpm-kinase dead (kd), or mock was cotransfected with TAp73 $\alpha$  and any one of FLAG-tagged YAP2-wt, YAP2-S127A, YAP2-1WW\*, YAP2-2WW\*, or mock into 293T cells by FuGENE-HD reagent. Four rows of lanes from the top in this order represent Western blotting with anti-HA, anti-FLAG, anti-p73, and antiactin in cell lysates. Two independent experiments were performed and representative data are shown.

April 16, 2007), we thought that another p53 family member, presumably transcriptionally active p73 (TAp73), should function in the induction of p21 and PUMA in these cells. p73 is able to bind promoters of several p53 responsive genes involved in cell cycle arrest and apoptosis including p21 and PUMA.<sup>61</sup> Unlike p53, it is rarely mutated or deleted in human malignant cells.<sup>62,63</sup> In addition, it has been reported that knockdown of p73 leads to enhanced resistance to DNA damage-inducing agents including DXR, ETP, and cisplatin.<sup>64</sup> Protein levels of p73 are kept low due to rapid degradation through the ubiquitin pathway under physiological conditions,<sup>65</sup> whereas TAp73 accumulates in response to stress caused by DNA damage.<sup>66</sup> Therefore, we regarded p73 as a p53-substituting molecule that mediated induction of p21 and PUMA, and examined the amount and the distribution of p73 in Kpm/Lats2-knockdown KG-1a cells and in control cells after treatment with ETP. As expected, after treatment of ETP, p73 protein level was kept very low in Kpm/Lats2-knockdown KG-1a cells compared with control cells, despite no difference in the mRNA level of p73. Immunofluorescence microscopic analysis revealed that nuclear accumulation of p73 was clearly detected in control cells but not, or only faintly, in Kpm/Lats2-knockdown cells. These results suggest that Kpm/Lats2 is involved in the stability and the nuclear accumulation of p73.

It has been shown that several steps are required for DNA damage-induced activation and stabilization of p73. DNA damage induces p73 gene expression via Chk1,<sup>67</sup> Chk2,<sup>68</sup> and E2F1.<sup>69,70</sup> and in parallel activates c-Abl and p38 MAP kinase (MAPK). Activated c-Abl and p38 MAPK phosphorylates p73 at Tyr99 and at Ser/Thr-Pro, respectively, to stabilize it in the nucleus.<sup>71-74</sup> In addition to phosphorylation, binding of phosphorylated p73 to promyelocytic leukemia protein (PML),<sup>65</sup> acetylation of p73 mediated by p300,<sup>75</sup> and prolyl isomerization of p73 mediated by peptidyl-prolyl *cis/trans* isomerase Pin1<sup>76</sup> are essential for functional activation of p73. YAP is essential for coactivation of p73 with PML and for recruitment of p300 and contributes to the DNA damage-induced nuclear accumulation of p73. Trapping of YAP in the cytosol due to phosphorylation by Akt (protein kinase B) and binding to 14-3-3 represents a physiological mechanism for the inhibition of inappropriately accumulated p73.<sup>77,78</sup> Among these factors, we concentrated our efforts on YAP because it should mediate the downstream signals of Kpm/Lats2 based on the analogy of *Drosophila*. We confirmed that Kpm/Lats2 could

interact with YAP2 through its first WW domain and induce phosphorylation of YAP2, which indicates that the Hpo-Wts-Yki axis is evolutionally conserved. However, the downstream signals of YAP (Yki) in mammals may be different from that in *Drosophila*, because, as mentioned in "Introduction," YAP has dual and opposite functions, growth-promoting or proapoptotic. In addition, as shown in this study, no alterations of the IAP family members were detected in Kpm/Lats2-knockdown cells, although Diap1 is considered to be one of the final target molecules in the *Drosophila* Hippo pathway. There is no report describing YAP-dependent regulation of the IAP family members in mammalian cells.

With regard to the relationship among Kpm/Lats2, YAP2, and p73, the transient expression experiments suggested that coexpression of Kpm/Lats2 positively regulates the protein amounts of both YAP2 and p73 in whole-cell lysates regardless of interaction with YAP2 via the WW domains and this effect requires phosphorylation of YAP2 at serine 127 by Kpm/Lats2. After submission of our original paper, Matallanas et al have reported that RASSF1A activates Lats1 through enhanced phosphorylation by MST2 and activated Lats1 phosphorylates and activates YAP1, allowing YAP1 to translocate to the nucleus and associate with p73, resulting in transcription of the proapoptotic target gene PUMA.<sup>79</sup> According to the authors, phosphorylation of YAP1 by Lats1 is needed to enable the formation of a YAP1-p73 complex, whereas, in unstimulated cells, Lats1 can negatively regulate YAP1 by sequestering YAP1 in the cytosol. Thus, it is suggested that Lats1 has dual functions as an anchoring protein that retains YAP1 in the cytosol and as a kinase that phosphorylates YAP1 to facilitate its interaction with p73. The former function has been emphasized by 2 recent papers insisting that inactivation of YAP by the Hippo pathway is involved in organ size control and cell contact inhibition.<sup>80,81</sup> These papers describe that Lats1 or Kpm/Lats2 but not AKT directly phosphorylates YAP at serine 127, increasing the interaction between YAP2 and 14-3-3. Our results are compatible with those with RASSF1A activation in that Lats1 or Kpm/Lats2 is crucial for the induction of proapoptotic gene PUMA that is mediated by the YAP-p73 complex. It should be noted that such function of Lats1 or Kpm/Lats2 becomes dominant only in the presence of proapoptotic stimulations such as RASSF1A activation, anti-Fas, and DNA damage-inducing agents. Evidence has indicated that DNA damage stress induces activation of c-Jun N-terminal kinase (JNK) and activated JNK then phosphorylates 14-3-3, resulting in release of

several 14-3-3-binding proteins including c-Abl, which is known to activate and stabilize p73 in the nucleus.<sup>82,83</sup> Thus, it seems possible that phosphorylation of 14-3-3 by activated JNK is involved in Kpm/Lats2-dependent nuclear translocation of YAP and accumulation of the YAP-p73 complex after DNA damage. Further studies are needed to clarify how DNA damage signals intersect the Hippo pathway.

In conclusion, we demonstrate that Kpm/Lats2 is required for the stabilization of p73 and subsequent induction of p21 and PUMA in response to DNA damage-inducing agents, suggesting that the down-regulation of Kpm/Lats2 contributes to the instability of p73 through the insufficient phosphorylation of YAP2 at serine 127, resulting in chemoresistance and poor prognosis for some leukemias.

## Acknowledgments

We thank Dr Masao Matsuoka and Dr Michiyuki Maeda (Laboratory of Virus Immunology, Research Center for AIDS, Institute for Virus Research, Kyoto University) for ATL-derived cell lines and the personal communication concerning ED-40515<sup>+</sup>; Dr Akira Nakagawara and Dr Toshinori Ozaki (Biochemistry, Chiba Cancer Center Research Institute, Chiba, Japan) for their experimental advice on p73; Dr Syohei Yamaoka for his help in preparation of

retrovirus vectors; Dr Yoshihide Ueda (Department of Gastroenterology and Hepatology, Kyoto University) for TAp73 $\alpha$ ; Virginia Mazack for expert technical assistance; and Dr Akifumi Takaori-Kondo (Department of Hematology and Oncology, Kyoto University) for the immunofluorescence microscope and his continuous help.

This work was supported in part by grants-in-aid from the Ministry of Education, Culture, Sports, Science, and Technology of Japan (T.H. and T.U.), and by a Pennsylvania Department of Health-sponsored Breast Cancer Research Grant (Philadelphia, PA; SAP no. 41-000-37378, M.S.).

## Authorship

Contribution: M.K. performed most experiments and cowrote the paper; T.H. designed the research and cowrote the paper; K.C. performed some experiments; T.O. and M.S. contributed vital plasmids; and T.U. supervised the research.

Conflict-of-interest disclosure: The authors declare no competing financial interests.

Correspondence: Toshiyuki Hori, Department of Hematology and Oncology, Graduate School of Medicine, Kyoto University, 54 Shogoin-Kawara-cho, Sakyo-ku, Kyoto 606-8507, Japan; e-mail: thori@kuhp.kyoto-u.ac.jp.

## References

- Justice RW, Zilian O, Woods DF, Noll M, Bryant PJ. The *Drosophila* tumor suppressor gene *warts* encodes a homolog of human myotonic dystrophy kinase and is required for the control of cell shape and proliferation. *Genes Dev.* 1995;9:534-546.
- Xu T, Wang W, Zhang S, Stewart RA, Yu W. Identifying tumor suppressors in genetic mosaics: the *Drosophila* *lats* gene encodes a putative protein kinase. *Development.* 1995;121:1053-1063.
- Edgar BA. From cell structure to transcription: Hippo forges a new path. *Cell.* 2006;124:267-273.
- Harvey K, Tapon N. The Salvador-Warts-Hippo pathway: an emerging tumour-suppressor network. *Nat Rev Cancer.* 2007;7:182-191.
- Pan D. Hippo signaling in organ size control. *Genes Dev.* 2007;21:886-897.
- Harvey KF, Pfleger CM, Hariharan IK. The *Drosophila* Mst ortholog, hippo, restricts growth and cell proliferation and promotes apoptosis. *Cell.* 2003;114:457-467.
- Huang J, Wu S, Barrera J, Matthews K, Pan D. The Hippo signaling pathway coordinately regulates cell proliferation and apoptosis by inactivating Yorkie, the *Drosophila* Homolog of YAP. *Cell.* 2005;122:421-434.
- Tapon N, Harvey KF, Bell DW, et al. *salvador* promotes both cell cycle exit and apoptosis in *Drosophila* and is mutated in human cancer cell lines. *Cell.* 2002;110:467-478.
- Wu S, Huang J, Dong J, Pan D. *hippo* encodes a Ste-20 family protein kinase that restricts cell proliferation and promotes apoptosis in conjunction with *salvador* and *warts*. *Cell.* 2003;114:445-456.
- He Y, Emoto K, Fang X, et al. *Drosophila* Mob family proteins interact with the related tricorned (Trc) and *warts* (Wts) kinases. *Mol Biol Cell.* 2005;16:4139-4152.
- Lai ZC, Wei X, Shimizu T, et al. Control of cell proliferation and apoptosis by mob as tumor suppressor, *mats*. *Cell.* 2005;120:675-685.
- Wei X, Shimizu T, Lai ZC. Mob as tumor suppressor is activated by Hippo kinase for growth inhibition in *Drosophila*. *EMBO J.* 2007;26:1772-1781.
- Hamaratoglu F, Willecke M, Kango-Singh M, et al. The tumour-suppressor genes NF2/Merlin and Expanded act through Hippo signalling to regulate cell proliferation and apoptosis. *Nat Cell Biol.* 2006;8:27-36.
- Bennett FC, Harvey KF. Fat cadherin modulates organ size in *Drosophila* via the Salvador/Warts/Hippo signaling pathway. *Curr Biol.* 2006;16:2101-2110.
- Cho E, Feng Y, Rauskolb C, Maitra S, Fehon R, Irvine KD. Delineation of a Fat tumor suppressor pathway. *Nat Genet.* 2006;38:1142-1150.
- Silva E, Tsatskis Y, Gardano L, Tapon N, McNeill H. The tumor-suppressor gene fat controls tissue growth upstream of expanded in the hippo signaling pathway. *Curr Biol.* 2006;16:2081-2089.
- Willecke M, Hamaratoglu F, Kango-Singh M, et al. The fat cadherin acts through the hippo tumor-suppressor pathway to regulate tissue size. *Curr Biol.* 2006;16:2090-2100.
- Hori T, Takaori-Kondo A, Kamikubo Y, Uchiyama T. Molecular cloning of a novel human protein kinase, *kpm*, that is homologous to *warts/lats*, a *Drosophila* tumor suppressor. *Oncogene.* 2000;19:3101-3109.
- Yabuta N, Fujii T, Copeland NG, et al. Structure, expression, and chromosome mapping of LATS2, a mammalian homologue of the *Drosophila* tumor suppressor gene *lats/warts*. *Genomics.* 2000;63:263-270.
- Kamikubo Y, Takaori-Kondo A, Uchiyama T, Hori T. Inhibition of cell growth by conditional expression of *kpm*, a human homologue of *Drosophila* *warts/lats* tumor suppressor. *J Biol Chem.* 2003;278:17609-17614.
- Li Y, Pei J, Xia H, Ke H, Wang H, Tao W. Lats2, a putative tumor suppressor, inhibits G1/S transition. *Oncogene.* 2003;22:4398-4405.
- Ke H, Pei J, Ni Z, et al. Putative tumor suppressor Lats2 induces apoptosis through downregulation of Bcl-2 and Bcl-x(L). *Exp Cell Res.* 2004;298:329-338.
- Aylon Y, Michael D, Shmueli A, Yabuta N, Nojima H, Oren M. A positive feedback loop between the p53 and Lats2 tumor suppressors prevents tetraploidization. *Genes Dev.* 2006;20:2687-2700.
- Kostic C, Shaw PH. Isolation and characterization of sixteen novel p53 response genes. *Oncogene.* 2000;19:3978-3987.
- Colombani J, Polesello C, Josue F, Tapon N. Dmp53 activates the Hippo pathway to promote cell death in response to DNA damage. *Curr Biol.* 2006;16:1453-1458.
- McPherson JP, Tamlyn L, Elia A, et al. Lats2/Kpm is required for embryonic development, proliferation control and genomic integrity. *EMBO J.* 2004;23:3677-3688.
- Yabuta N, Okada N, Ito A, et al. Lats2 is an essential mitotic regulator required for the coordination of cell division. *J Biol Chem.* 2007;282:19259-19271.
- Chan EH, Nousiainen M, Chalamalasetty RB, Schafer A, Nigg EA, Sillje HH. The Ste20-like kinase Mst2 activates the human large tumor suppressor kinase Lats1. *Oncogene.* 2005;24:2076-2086.
- Sudol M. Yes-associated protein (YAP65) is a proline-rich phosphoprotein that binds to the SH3 domain of the Yes proto-oncogene product. *Oncogene.* 1994;9:2145-2152.
- Sudol M, Bork P, Einbond A, et al. Characterization of the mammalian YAP (Yes-associated protein) gene and its role in defining a novel protein module, the WW domain. *J Biol Chem.* 1995;270:14733-14741.
- Macias MJ, Wiesner S, Sudol M. WW and SH3 domains, two different scaffolds to recognize proline-rich ligands. *FEBS Lett.* 2002;513:30-37.
- Vassilev A, Kaneko KJ, Shu H, Zhao Y, DePamphilis ML. TEAD/TEF transcription factors utilize the activation domain of YAP65, a Src/Yes-associated protein localized in the cytoplasm. *Genes Dev.* 2001;15:1229-1241.
- Komuro A, Nagai M, Navin NE, Sudol M. WW domain-containing protein YAP associates with ErbB-4 and acts as a co-transcriptional activator for the carboxyl-terminal fragment of ErbB-4 that translocates to the nucleus. *J Biol Chem.* 2003;278:33334-33341.

34. Aqeilan RI, Donati V, Palamarchuk A, et al. WW domain-containing proteins, WWOX and YAP, compete for interaction with ErbB-4 and modulate its transcriptional function. *Cancer Res*. 2005;65:6764-6772.
35. Yagi R, Chen LF, Shigesada K, Murakami Y, Ito Y. A WW domain-containing yes-associated protein (YAP) is a novel transcriptional co-activator. *EMBO J*. 1999;18:2551-2562.
36. Zaidi SK, Sullivan AJ, Medina R, et al. Tyrosine phosphorylation controls Runx2-mediated subnuclear targeting of YAP to repress transcription. *EMBO J*. 2004;23:790-799.
37. Overholtzer M, Zhang J, Smolen GA, et al. Transforming properties of YAP, a candidate oncogene on the chromosome 11q22 amplicon. *Proc Natl Acad Sci U S A*. 2006;103:12405-12410.
38. Zender L, Spector MS, Xue W, et al. Identification and validation of oncogenes in liver cancer using an integrative oncogenomic approach. *Cell*. 2006;125:1253-1267.
39. Espanel X, Sudol M. Yes-associated protein and p53-binding protein-2 interact through their WW and SH3 domains. *J Biol Chem*. 2001;276:14514-14523.
40. Samuels-Lev Y, O'Connor DJ, Bergamaschi D, et al. ASPP proteins specifically stimulate the apoptotic function of p53. *Mol Cell*. 2001;8:781-794.
41. Dobbstein M, Strano S, Roth J, Blandino G. p73-induced apoptosis: a question of compartments and cooperation. *Biochem Biophys Res Commun*. 2005;331:688-693.
42. Takahashi Y, Miyoshi Y, Takahata C, et al. Downregulation of LATS1 and LATS2 mRNA expression by promoter hypermethylation and its association with biologically aggressive phenotype in human breast cancers. *Clin Cancer Res*. 2005;11:1380-1385.
43. Jiménez-Velasco A, Roman-Gomez J, Agirre X, et al. Downregulation of the large tumor suppressor 2 (LATS2/KPM) gene is associated with poor prognosis in acute lymphoblastic leukemia. *Leukemia*. 2005;19:2347-2350.
44. Koeffler HP, Billing R, Lusa AJ, Sparkes R, Golde DW. An undifferentiated variant derived from the human acute myelogenous leukemia cell line (KG-1). *Blood*. 1980;56:265-273.
45. Maeda M, Arima N, Daitoku Y, et al. Evidence for the interleukin-2 dependent expansion of leukemic cells in adult T cell leukemia. *Blood*. 1987;70:1407-1411.
46. Ohno Y, Amakawa R, Fukuhara S, et al. Acute transformation of chronic large granular lymphocyte leukemia associated with additional chromosome abnormality. *Cancer*. 1989;64:63-67.
47. Kawahara M, Hori T, Matsubara Y, Okawa K, Uchiyama T. Identification of HLA class I-restricted tumor-associated antigens in adult T cell leukemia cells by mass spectrometric analysis. *Exp Hematol*. 2006;34:1496-1504.
48. Matsubar Y, Hori T, Morita R, Sakaguchi S, Uchiyama T. Delineation of immunoregulatory properties of adult T-cell leukemia cells. *Int J Hematol*. 2006;84:63-69.
49. Ueda Y, Hijikata M, Takagi S, Chiba T, Shimotohno K. New p73 variants with altered C-terminal structures have varied transcriptional activities. *Oncogene*. 1999;18:4993-4998.
50. National Center for Biotechnology Information. BLASTN. <http://www.ncbi.nlm.nih.gov/blast/Blast.cgi?PAGE=Nucleotides&PROGRAM=blastn>. Accessed on March 11, 2005.
51. Rocco JW, Leong CO, Kuperwasser N, DeYoung MP, Ellisen LW. p63 mediates survival in squamous cell carcinoma by suppression of p73-dependent apoptosis. *Cancer Cell*. 2006;9:45-56.
52. Voorhoeve PM, le Sage C, Schrier M, et al. A genetic screen implicates miRNA-372 and miRNA-373 as oncogenes in testicular germ cell tumors. *Cell*. 2006;124:1169-1181.
53. Clave E, Carosella ED, Gluckman E, Socie G. Radiation-enhanced expression of interferon-inducible genes in the KG1a primitive hematopoietic cell line. *Leukemia*. 1997;11:114-119.
54. Weiss RH. p21Waf1/Cip1 as a therapeutic target in breast and other cancers. *Cancer Cell*. 2003;4:425-429.
55. Yu J, Zhang L. No PUMA, no death: implications for p53-dependent apoptosis. *Cancer Cell*. 2003;4:248-249.
56. Kim H, Rafiuddin-Shah M, Tu HC, et al. Hierarchical regulation of mitochondrion-dependent apoptosis by BCL-2 subfamilies. *Nat Cell Biol*. 2006;8:1348-1358.
57. Nachmias B, Ashhab Y, Ben-Yehuda D. The inhibitor of apoptosis protein family (IAPs): an emerging therapeutic target in cancer. *Semin Cancer Biol*. 2004;14:231-243.
58. Ozaki T, Nakagawara A. p73, a sophisticated p53 family member in the cancer world. *Cancer Sci*. 2005;96:729-737.
59. Jiang Z, Li X, Hu J, et al. Promoter hypermethylation-mediated down-regulation of LATS1 and LATS2 in human astrocytoma. *Neurosci Res*. 2006;56:450-458.
60. Sherr CJ, Roberts JM. Inhibitors of mammalian G1 cyclin-dependent kinases. *Genes Dev*. 1995;9:1149-1163.
61. Melino G, De Laurenzi V, Vousden KH. p73: friend or foe in tumorigenesis. *Nat Rev Cancer*. 2002;2:605-615.
62. Ichimiya S, Nimura Y, Kageyama H, et al. p73 at chromosome 1p36.3 is lost in advanced stage neuroblastoma but its mutation is infrequent. *Oncogene*. 1999;18:1061-1066.
63. Pluta A, Nyman U, Joseph B, Robak T, Zhivotovskiy B, Smolewski P. The role of p73 in hematological malignancies. *Leukemia*. 2006;20:757-766.
64. Irwin MS, Kondo K, Marin MC, Cheng LS, Hahn WC, Kaelin WG Jr. Chemosensitivity linked to p73 function. *Cancer Cell*. 2003;3:403-410.
65. Bernassola F, Salomoni P, Oberst A, et al. Ubiquitin-dependent degradation of p73 is inhibited by PML. *J Exp Med*. 2004;199:1545-1557.
66. Rossi M, De Laurenzi V, Munariz E, et al. The ubiquitin-protein ligase Itch regulates p73 stability. *EMBO J*. 2005;24:836-848.
67. Gonzalez S, Prives C, Cordon-Cardo C. p73alpha regulation by Chk1 in response to DNA damage. *Mol Cell Biol*. 2003;23:8161-8171.
68. Urist M, Tanaka T, Poyurovsky MV, Prives C. p73 induction after DNA damage is regulated by checkpoint kinases Chk1 and Chk2. *Genes Dev*. 2004;18:3041-3054.
69. Irwin M, Marin MC, Phillips AC, et al. Role for the p53 homologue p73 in E2F-1-induced apoptosis. *Nature*. 2000;407:645-648.
70. Stiewe T, Putzer BM. Role of the p53-homologue p73 in E2F1-induced apoptosis. *Nat Genet*. 2000;26:464-469.
71. Agami R, Blandino G, Oren M, Shaul Y. Interaction of c-Abl and p73alpha and their collaboration to induce apoptosis. *Nature*. 1999;399:809-813.
72. Gong JG, Costanzo A, Yang HQ, et al. The tyrosine kinase c-Abl regulates p73 in apoptotic response to cisplatin-induced DNA damage. *Nature*. 1999;399:806-809.
73. Yuan ZM, Shioya H, Ishiko T, et al. p73 is regulated by tyrosine kinase c-Abl in the apoptotic response to DNA damage. *Nature*. 1999;399:814-817.
74. Sanchez-Prieto R, Rojas JM, Taya Y, Gutkind JS. A role for the p38 mitogen-activated protein kinase pathway in the transcriptional activation of p53 on genotoxic stress by chemotherapeutic agents. *Cancer Res*. 2000;60:2464-2472.
75. Costanzo A, Merio P, Pediconi N, et al. DNA damage-dependent acetylation of p73 dictates the selective activation of apoptotic target genes. *Mol Cell*. 2002;9:175-186.
76. Mantovani F, Piazza S, Gostissa M, et al. Pin1 links the activities of c-Abl and p300 in regulating p73 function. *Mol Cell*. 2004;14:625-636.
77. Basu S, Totty NF, Irwin MS, Sudol M, Downward J. Akt phosphorylates the Yes-associated protein, YAP, to induce interaction with 14-3-3 and attenuation of p73-mediated apoptosis. *Mol Cell*. 2003;11:11-23.
78. Strano S, Monti O, Pediconi N, et al. The transcriptional coactivator Yes-associated protein drives p73 gene-target specificity in response to DNA Damage. *Mol Cell*. 2005;18:447-459.
79. Matallanas D, Romano D, Yee K, et al. RASSF1A elicits apoptosis through an MST2 pathway directing proapoptotic transcription by the p73 tumor suppressor protein. *Mol Cell*. 2007;27:962-975.
80. Dong J, Feldmann G, Huang J, et al. Elucidation of a universal size-control mechanism in Drosophila and mammals. *Cell*. 2007;130:1120-1133.
81. Zhao B, Wei X, Li W, et al. Inactivation of YAP oncoprotein by the Hippo pathway is involved in cell contact inhibition and tissue growth control. *Genes Dev*. 2007;21:2747-2761.
82. Yoshida K, Yamaguchi T, Natsume T, Kufe D, Miki Y. JNK phosphorylation of 14-3-3 proteins regulates nuclear targeting of c-Abl in the apoptotic response to DNA damage. *Nat Cell Biol*. 2005;7:278-285.
83. Sunayama J, Tsuruta F, Masuyama N, Gotoh Y. JNK antagonizes Akt-mediated survival signals by phosphorylating 14-3-3. *J Cell Biol*. 2005;170:295-304.

# Ozone production by amino acids contributes to killing of bacteria

Kouhei Yamashita<sup>a,1</sup>, Takashi Miyoshi<sup>a</sup>, Toshiyuki Arai<sup>b</sup>, Nobuyuki Endo<sup>c</sup>, Hiroshi Itoh<sup>d</sup>, Keisuke Makino<sup>e</sup>, Kiyomi Mizugishi<sup>f</sup>, Takashi Uchiyama<sup>a</sup>, and Masataka Sasada<sup>d</sup>

Departments of <sup>a</sup>Hematology and Oncology and <sup>b</sup>Anesthesia, Kyoto University Hospital, Kyoto 606-8507, Japan; <sup>c</sup>Wakasa Wan Energy Research Center, Tsuruga, Fukui 914-0129, Japan; <sup>d</sup>Human Health Sciences, Graduate School of Medicine, Kyoto University, Kyoto 606-8507, Japan; <sup>e</sup>Institute of Advanced Energy, Kyoto University, Uji, Kyoto 611-0011, Japan; and <sup>f</sup>Department of Physiology, Kanazawa University Graduate School of Medical Sciences, Kanazawa, Ishikawa 920-8640, Japan

Edited by Richard A. Lerner, The Scripps Research Institute, La Jolla, CA, and approved September 18, 2008 (received for review August 12, 2008)

**Reactive oxygen species produced by phagocytosing neutrophils are essential for innate host defense against invading microbes. Previous observations revealed that antibody-catalyzed ozone formation by human neutrophils contributed to the killing of bacteria. In this study, we discovered that 4 amino acids themselves were able to catalyze the production of an oxidant with the chemical signature of ozone from singlet oxygen in the water-oxidation pathway, at comparable level to antibodies. The resultant oxidant with the chemical signature of ozone exhibited significant bactericidal activity in our distinct cell-free system and in human neutrophils. The results also suggest that an oxidant with the chemical signature of ozone produced by neutrophils might potentiate a host defense system, when the host is challenged by high doses of infectious agents. Our findings provide biological insights into the killing of bacteria by neutrophils.**

host defense | singlet oxygen | neutrophil | chronic granulomatous disease

Neutrophils are one of the professional phagocytes, which ingest microorganisms into intracellular compartments called phagosomes, and destroy them. The production of reactive oxygen species (ROS) by phagocytosing neutrophils is essential for innate host defense against invading microbial pathogens. The phagocytosing neutrophils undergo a burst of oxygen consumption that is caused by the reduced NADPH oxidase, ultimately leading to the formation of hypochlorous acid (HOCl), singlet oxygen (<sup>1</sup>O<sub>2</sub>), and hydroxyl radical (<sup>•</sup>OH). However, a clear scenario of how the ROS kill microbes has not yet emerged (1). Recently, it has been proposed that neutrophils produce ozone, which likely contributes to the bactericidal and inflammatory activity of neutrophils (2–4), although the validity of this model is still a matter of debate (5, 6). In this model, antibodies can catalyze the production of ozone from singlet oxygen and water, but the precise mechanism of how antibodies achieve this reaction remains uncertain.

Chronic granulomatous disease (CGD) is characterized by a defect in ROS formation, leading to recurrent, often life-threatening bacterial and fungal infections, and granuloma formation in multiple organs. The disease is caused by a genetic mutation in 1 of 4 components of NADPH oxidase (gp91-*phox*, p47-*phox*, p67-*phox*, and p22-*phox*) of the superoxide (O<sub>2</sub><sup>•-</sup>)-generating phagocytes (7). Patients with a defect in the gp91-*phox* component, which is the most common type of CGD (≈60%), are reported to exhibit a more severe clinical course than those with a defect in the p47-*phox* component (8). Recently, we experienced a patient with a rare variant type of CGD carrying a defect in the gp91-*phox* component. Despite the genetic defect, his granulocytes could produce significant amounts of singlet oxygen, but very little superoxide. Thus, neutrophils from this CGD patient would provide a useful model system in humans. In this study, we investigated the biological importance of ozone produced by human neutrophils by using

the variant CGD neutrophils and our distinct in vitro assay system.

## Results

**Ozone Production by Immunoglobulins and Amino Acids in the Cell-Free System.** In our current study, we explored the mechanism by which antibodies produce ozone from singlet oxygen and water. We previously established a cell-free system, in which 6-formylpterin (6FP), a potent xanthine oxidase inhibitor, produces singlet oxygen without superoxide formation under UVA radiation in aqueous solutions (9). Using this system, we found that the portion of F(ab')<sub>2</sub> of antibodies, albumin, and chemotactic peptide, formyl-methionyl-leucyl-phenylalanine (FMLP), had the potential to generate an oxidant with the chemical signature of ozone, as intact antibodies (IgG) did, as denoted by the oxidation reaction of indigo carmine to isatin sulfonic acids, detected by a spectrophotometric assay (Fig. 1A). However, an inhibitory peptide of caspases, benzyloxycarbonyl-Val-Ala-Asp(OMe)-fluoromethylketone (zVAD-fmk), did not produce an oxidant with the chemical signature of ozone (Fig. 1B). Furthermore, the addition of catalase, which catalyzes the decomposition of H<sub>2</sub>O<sub>2</sub> to H<sub>2</sub>O and O<sub>2</sub>, did not affect the generation of an oxidant with the chemical signature of ozone by IgG in this system (Fig. 1C). These results substantiate the previous observation by Wentworth *et al.* (2) and further suggest that the ozone generation brought about by antibodies is not attributable to the antigen-binding activity of antibodies. We further examined what components contribute to ozone production in this system. Surprisingly, among various water-soluble amino acids applied, 4 amino acids [tryptophan (Trp), methionine (Met), cysteine (Cys), and histidine (His)] exhibited catalytic activity sufficient for the conversion of singlet oxygen to an oxidant with the chemical signature of ozone in a dose-dependent manner (Fig. 1D and E). Scavengers of singlet oxygen, sodium azide and edaravone (10), significantly abrogated the ability of these amino acids to catalyze the reaction (Fig. 1F), whereas catalase had no effects on the reaction (Fig. 1G), suggesting the specificity of this assay system. To further verify the amino acid-catalyzed ozone generation, we performed HPLC assay for detection of isatin sulfonic acid (Fig. 2A and B) and 4-carboxybenzaldehyde (Fig. 2C and D). The administration of Met to 6FP under UVA radiation successfully converted indigo carmine (Fig. 2A) to isatin sulfonic acid (Fig. 2B). Moreover, another detector of ozone, vinylbenzoic acid (Fig. 2C), was oxidized to 4-carboxybenzaldehyde (Fig. 2D), support-

Author contributions: K.Y., T.U., and M.S. designed research; K.Y., T.M., T.A., N.E., and H.I. performed research; K. Makino contributed new reagents/analytic tools; K.Y. analyzed data; and K.Y. and K. Mizugishi wrote the paper.

The authors declare no conflict of interest.

This article is a PNAS Direct Submission.

<sup>1</sup>To whom correspondence should be addressed. E-mail: kouhei@kuhp.kyoto-u.ac.jp.

© 2008 by The National Academy of Sciences of the USA

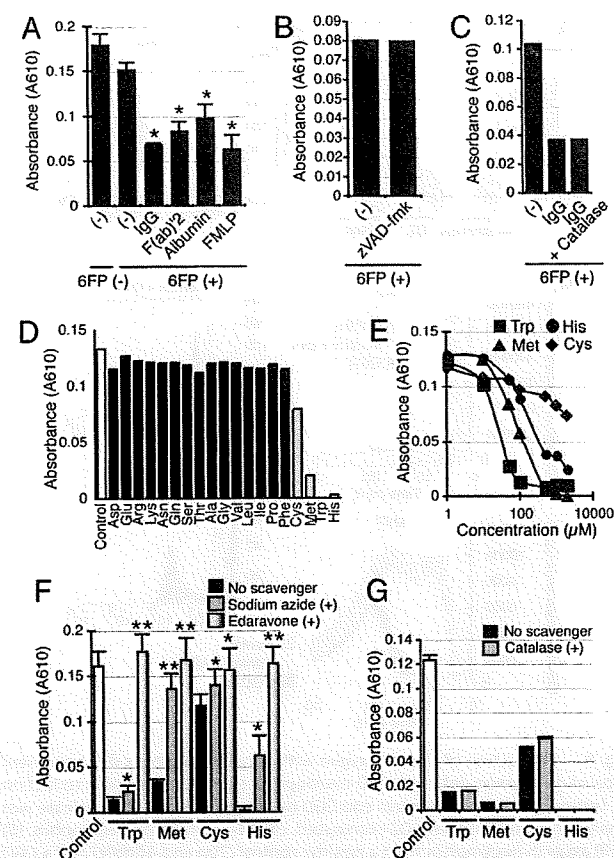


**Fig. 1.** Ozone production by immunoglobulins and amino acids in the cell-free system. Indigo carmine was irradiated with UVA in the presence of 6FP. An oxidant with the chemical signature of ozone produced by the addition of immunoglobulins or amino acids converted indigo carmine to isatin sulfonic acids. Loss of indigo carmine was monitored by measuring its absorbance at 610 nm. (A) Effect of Ig, the portion of F(ab)<sub>2</sub> of antibodies, albumin, or FMLP in the presence of 6FP on ozone production. The data represent mean values  $\pm$  SD ( $n = 3$ ; \*,  $P < 0.05$ , paired  $t$  test). (B) Effect of zVAD-fmk in the presence of 6FP on ozone production. The experiments were performed at least 3 times, and representative data are shown. (C) Effect of catalase in the presence of 6FP on IgG-mediated ozone production. The experiments were performed at least 3 times, and representative data are shown. (D) Effect of water-soluble amino acids in the presence of 6FP on ozone production. Representative data are shown. (E) Dose-response curves. Increasing concentrations of Trp, Met, Cys, or His (1  $\mu$ M to 2 mM) were added to the reaction in the presence of 6FP. (F) Effect of scavengers of singlet oxygen, sodium azide, and edaravone on amino acid (Trp, Met, Cys, or His)-mediated ozone production. The data represent mean values  $\pm$  SD ( $n = 3$ ; \*,  $P < 0.05$ ; \*\*,  $P < 0.01$ ; paired  $t$  test). (G) Effect of catalase on amino acid (Trp, Met, Cys, or His)-mediated ozone production. The data represent mean values  $\pm$  SD ( $n = 3$ ).

ing the formation of an oxidant with the chemical signature of ozone by amino acids. The amino acids-catalyzed ozone generation was further confirmed by measuring <sup>18</sup>O incorporation from the reaction solvent H<sub>2</sub><sup>18</sup>O into isatin sulfonic acid during indigo carmine oxidation by using mass spectral analysis. In a control experiment, where normal H<sub>2</sub><sup>16</sup>O was used in the presence of Met and 6FP with UVA irradiation, the mass peak 226 was detected, suggesting that isatin sulfonic acid was produced in the system (Fig. 2E). Mass spectral profile with H<sub>2</sub><sup>18</sup>O revealed that the additional mass peak 230, which is characteristic of ozone (2), was observed when Met and 6FP in a reaction mixture containing H<sub>2</sub><sup>18</sup>O were irradiated with UVA (Fig. 2G), whereas the mass peak 226 and 228 alone were observed in the

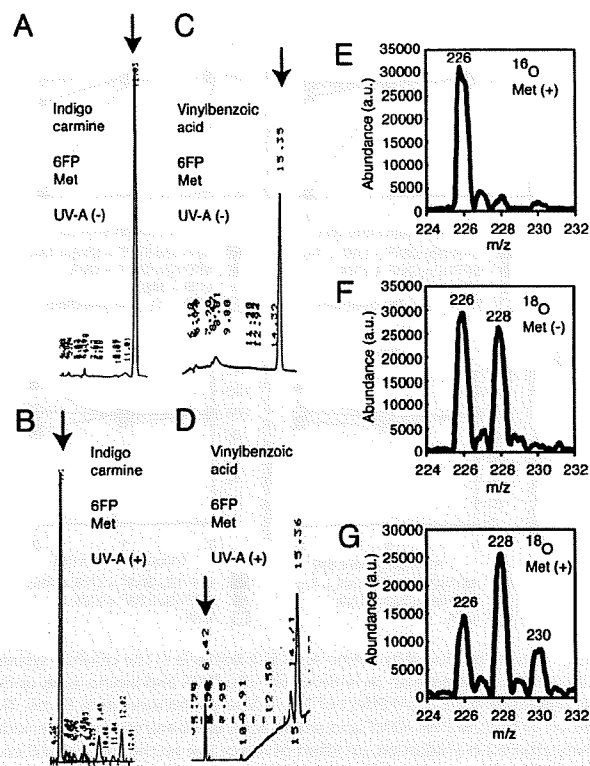


**Fig. 2.** HPLC and mass spectral analysis of ozone production in the cell-free system. (A and B) HPLC analysis. Indigo carmine was added to 6FP and Met with (B) or without (A) UVA irradiation. Arrows indicate a peak of indigo carmine (A) and isatin sulfonic acid (B). (C and D) HPLC analysis. Vinylbenzoic acid was added to 6FP and Met with (D) or without (C) UVA irradiation. Arrows indicate a peak of vinylbenzoic acid (C) and 4-carboxybenzaldehyde (D). (E–G) Mass spectral analysis. Indigo carmine was added to 6FP in a reaction mixture containing H<sub>2</sub><sup>16</sup>O in the presence of Met (E), H<sub>2</sub><sup>16</sup>O in the absence (F) or presence (G) of Met and irradiated with UVA. Note the presence of the mass peak 230 in G.

absence of Met (Fig. 2F). These results demonstrate that the oxidant-carrying chemical signature of ozone was produced in our amino acids-mediated water oxidation pathway.

**Ozone Produced by Amino Acids Exhibits Bactericidal Activity in the Cell-Free System.** We next investigated whether an oxidant with the chemical signature of ozone produced by amino acids killed bacteria in our cell-free system. Bactericidal studies were performed on catalase-positive bacteria, *Escherichia coli*, NIHJ-JC2. In this experiment, to increase solubility in water, we used a variant of 6FP, 2-(N,N-dimethylaminomethyleneamino)-6-formyl-3-pivaloylpteridine-4-one (6FP-tBu-DMF), which generates singlet oxygen to a similar extent to 6FP (9). Viable *E. coli* were nearly undetectable with the addition of 6FP-tBu-DMF and amino acids (Trp or Met) after a 2-h irradiation, whereas 6FP-tBu-DMF alone had little effect on the viability of *E. coli* even with a 2-h irradiation (Fig. 3A). The administration of IgG together with 6FP-tBu-DMF exhibited a similar profile to these amino acids (data not shown). These results provide evidence to support the key role of these amino acids in bactericidal activity. The viability of *E. coli* was not affected by the addition of Arg or Phe, which had failed to exhibit catalytic activity for the generation of an oxidant with the chemical signature of ozone (Fig. 3B). Given that hydrogen peroxide (H<sub>2</sub>O<sub>2</sub>), which is highly bactericidal, is also the ultimate product of the water-oxidation pathway, it is rational to speculate that H<sub>2</sub>O<sub>2</sub> might mediate the



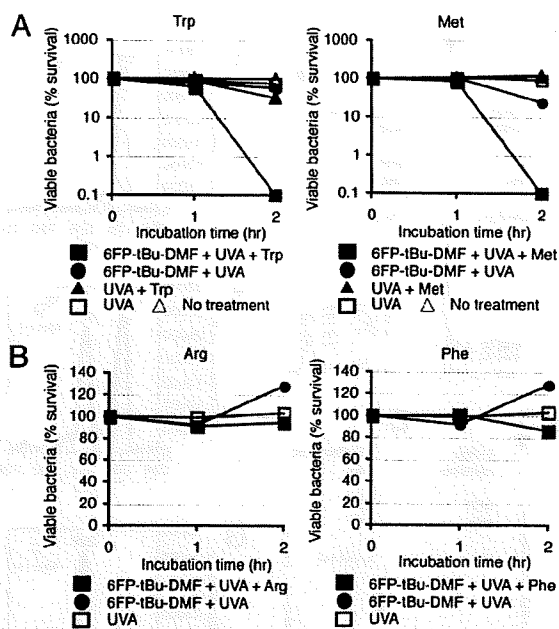


**Fig. 3.** Ozone produced by amino acids kills bacteria in the cell-free system. *E. coli* were incubated with or without 6FP-tBu-DMF and amino acids under UVA irradiation for 2 h. (A) Effect of Trp or Met on the survival of *E. coli*. The addition of both 6FP-tBu-DMF and amino acids exhibited strong bactericidal activity after a 2-h irradiation. (B) Effect of Arg or Phe on the survival of *E. coli*. Note that the amino acids showed no effects on bactericidal activity.

bactericidal activity observed. Quantification of  $H_2O_2$  toxicity against *E. coli* revealed that  $H_2O_2$  levels on treatment with 6FP-tBu-DMF and amino acids were  $\approx 80 \mu M$ , which was completely repressed by catalase treatment (Fig. 4A). However,  $H_2O_2$  levels required to kill 50% of the bacteria were  $\approx 1-10$  mM (Fig. 4B), suggesting that  $H_2O_2$  is unlikely to be the principal contributor to the killing activity in this system.

**Ozone Production by Amino Acids in Human Neutrophils.** Next, we examined whether human neutrophils really have the functional capacity to produce ozone. We have identified a patient with a rare variant type of CGD carrying a defect in the gp91-phox component, whose granulocytes could produce significant amounts of singlet oxygen, but very little superoxide. Thus, neutrophils from this CGD patient should provide a useful model to allow the testing of our hypothesis in human neutrophils, because it is difficult to determine whether the amino

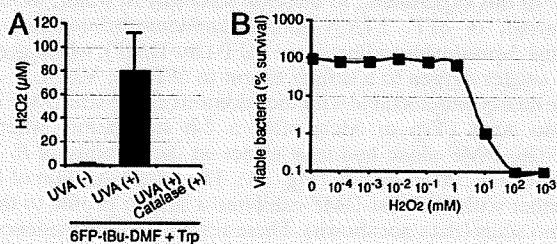


**Fig. 4.**  $H_2O_2$  levels in the cell-free system. (A)  $H_2O_2$  levels generated by 6FP-tBu-DMF and Trp after 2-h irradiation. Note that  $H_2O_2$  production was completely repressed by catalase treatment. The data represent mean values  $\pm$  SD ( $n = 3$ ). (B) Concentration-dependent toxicity of  $H_2O_2$  on the viability of *E. coli*. Increasing concentrations of  $H_2O_2$  ( $0-10^3$  mM) were added to the *E. coli*. The experiments were performed at least 3 times, and representative data are shown.

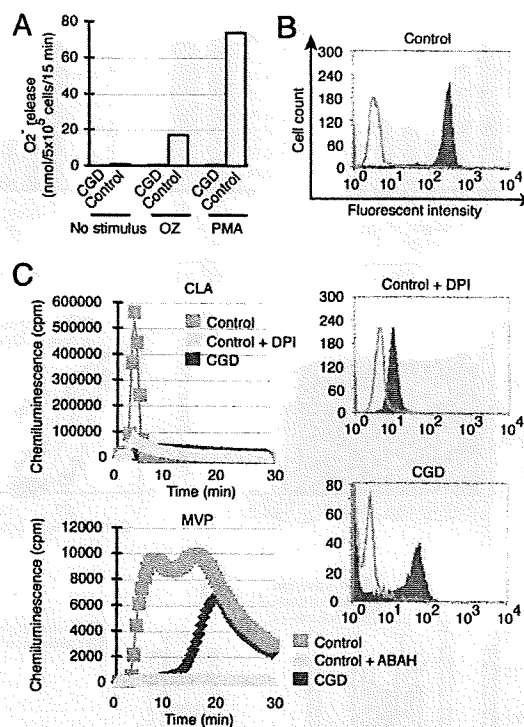


**Fig. 5.** Production of singlet oxygen with very little superoxide in a variant type of gp91-phox-deficient CGD neutrophils. (A) SOD-inhibitable reduction of ferricytochrome *c* in control and CGD neutrophils. Superoxide release was analyzed in unstimulated, OZ-stimulated, or PMA-stimulated neutrophils. (B) DHR assay in neutrophils from a healthy control (Top and Middle) and a CGD patient (Bottom). In Middle the pretreatment of control neutrophils with DPI, an inhibitor of NADPH-oxidase, is revealed. Fluorescence intensity is shown on the logarithmic x axis, and the cell count is shown on the y axis. (C) Superoxide (Upper) and singlet oxygen (Lower) release from control and CGD neutrophils. Neutrophils were incubated with CLA for superoxide detection or MVP for singlet oxygen detection, and luminescence was monitored every 30 s for 30 min. Some control neutrophils were pretreated with DPI for the CLA (Upper) or with ABAH, an inhibitor of MPO, for the MVA (Lower).

acid-catalyzed generation of ozone actually occurs *in vivo* by using healthy human neutrophils. Extracellular superoxide production was measured by the superoxide dismutase (SOD)-inhibitable reduction of ferricytochrome *c*. Neutrophils from a healthy control released substantial amounts of superoxide in response to stimulation with either phorbol myristate acetate (PMA) or opsonized zymosan (OZ). In sharp contrast, neutrophils from this CGD patient did not release detectable superoxide in response to either stimulus (Fig. 5A). We next used the fluorescent dye dihydrorhodamine (DHR) 123 in a flow cytometric assay to detect ROS. PMA-stimulated neutrophils from a healthy control revealed a significant increase in DHR fluorescence, which was counteracted by pretreatment with diphenyleneiodonium (DPI), an inhibitor of NADPH-oxidase (Fig. 5B). In contrast, neutrophils from the gp91-phox-mutated variant CGD patient exhibited a moderate fluorescence increase after PMA stimulation, reminiscent of the partial DHR response reported in p47-phox-deficient CGD patients (Fig. 5B) (11). To further verify the results, we used 2 chemiluminescent probes, 2-methyl-6-phenyl-3,7-dihydroimidazo[1,2-a]pyrazin-3-one (CLA) and *trans*-1-(2'-methoxyvinyl)pyrene (MVP), which were developed to specifically detect superoxide and singlet oxygen, respectively (10, 12-14). The pretreatment of control neutrophils with DPI abolished the CLA chemiluminescence, suggesting the specificity of this probe for superoxide detection (Fig. 5C). The

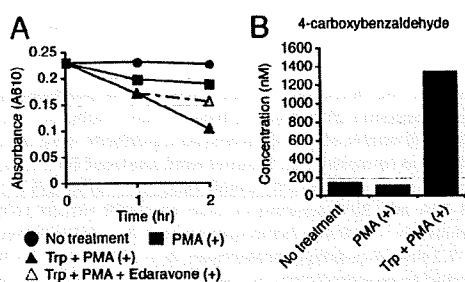


**Fig. 6.** Ozone production in a variant type of gp91-phox-deficient CGD neutrophils. (A) Effect of Trp on ozone production in activated CGD neutrophils. Indigo carmine was incubated with unstimulated or PMA-stimulated CGD neutrophils. Trp was added to PMA-stimulated CGD neutrophils to analyze ozone production. Loss of indigo carmine was monitored by measuring its absorbance at 610 nm. Note that a scavenger of singlet oxygen, edaravone, partially suppressed the reaction. The experiments were performed at least 3 times, and representative data are shown. (B) HPLC analysis of 4-carboxybenzaldehyde in CGD neutrophils. PMA-stimulated CGD neutrophils with Trp administration produced 4-carboxybenzaldehyde from vinylbenzoic acid.

treatment of control neutrophils with 4-aminobenzoic acid hydrazide (ABAH), an inhibitor of myeloperoxidase (MPO), abrogated the MVP chemiluminescence (Fig. 5C). The CLA chemiluminescence in the variant CGD neutrophils was nearly undetectable, whereas the MVA chemiluminescence in the CGD neutrophils was approximately half of that in healthy control neutrophils, suggesting that the variant CGD neutrophils produced very small amounts of superoxide, but had the ability to produce singlet oxygen to some extent (Fig. 5C). To verify our results in the cell-free system, an oxidation reaction of indigo carmine was carried out on neutrophils from the variant CGD patient. Spectrophotometric assay revealed that the addition of Trp to PMA-stimulated neutrophils led to the successful conversion of indigo carmine to isatin sulfonic acids (Fig. 6A). A scavenger of singlet oxygen, edaravone, partially suppressed the reaction (Fig. 6A). HPLC analysis revealed that the PMA-stimulated CGD neutrophils with Trp administration produced 4-carboxybenzaldehyde from vinylbenzoic acid (Fig. 6B), substantiating the production of an oxidant with the chemical signature of ozone from singlet oxygen in human neutrophils.

**Ozone Produced by Amino Acids Augments Bactericidal Activity of Human Neutrophils.** Finally, we examined the bactericidal activity of neutrophils from the variant CGD patient. A bactericidal assay revealed that the CGD neutrophils were able to partially kill *E. coli* in a condition whereby the ratio of neutrophils to *E. coli* was 1:1, although the killing activity was less than that of healthy neutrophils (Fig. 7A). In the variant CGD neutrophils, the administration of amino acids, Trp and Met, augmented the bactericidal activity of neutrophils, which was more evident when the ratio of *E. coli* to neutrophils was high (>5:1) (Fig. 7B and data not shown). These results suggest that the formation of an oxidant with the chemical signature of ozone catalyzed by amino acids facilitate the bactericidal action of the variant CGD neutrophils. This beneficial effect of amino acids on bactericidal activity was also observed in healthy neutrophils, when higher doses of *E. coli* were added to neutrophils (Fig. 7C and data not shown). These results are indicative of a general role for amino acid-catalyzed ozone in the bactericidal action of human neutrophils. To examine the effect of H<sub>2</sub>O<sub>2</sub> on the killing activity of neutrophils, we measured the H<sub>2</sub>O<sub>2</sub> concentration by using a highly sensitive and stable H<sub>2</sub>O<sub>2</sub> probe, *N*-acetyl-3,7,2-phenylethylamine dihydroxyphenoxazine (15). In contrast to healthy neutrophils, the H<sub>2</sub>O<sub>2</sub> level in the CGD neutrophils was

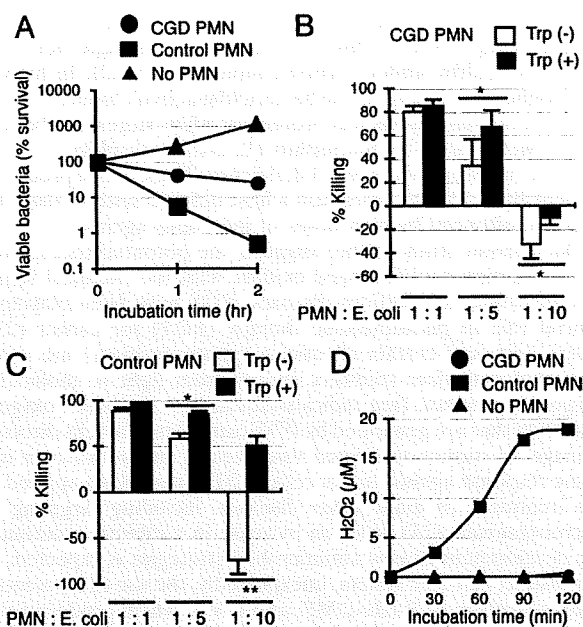


**Fig. 7.** Ozone produced by amino acids augments the bactericidal activity of neutrophils. (A) Bactericidal activity of CGD and healthy control neutrophils (PMN). *E. coli* were incubated with CGD or control neutrophils for 2 h. (B and C) Effect of Trp on the bactericidal activity of CGD (B) and healthy control (C) neutrophils. CGD or control neutrophils were challenged with increasing amounts of *E. coli* at a ratio of 1:1, 1:5, or 1:10 in the presence or absence of Trp. The data represent mean values  $\pm$  SD ( $n = 3$ ;  $P < 0.05$ ;  $**$ ,  $P < 0.01$ ; paired *t* test). (D) H<sub>2</sub>O<sub>2</sub> levels produced by CGD and healthy control neutrophils. The experiments were performed at least 3 times, and representative data are shown.

negligible, indicating that H<sub>2</sub>O<sub>2</sub> is unlikely to be relevant to the killing activity (Fig. 7D).

## Discussion

In this study, we showed that 4 amino acids, by themselves, were able to catalyze the production of an oxidant with the chemical signature of ozone from singlet oxygen in the water-oxidation pathway, comparably to antibodies. The resultant oxidant with the chemical signature of ozone exhibited significant bactericidal activity in our cell-free system and in human neutrophils. Ozone production by neutrophils is still a debatable issue. However, considering the findings of this study, where distinct model systems were exploited, we favor the proposal by Wentworth and colleagues (2–4) that antibodies can catalyze ozone generation in neutrophils. Our results further suggested the hypothesis that amino acids themselves exhibited catalytic activity to convert singlet oxygen and water to an oxidant with the chemical signature of ozone, and amino acid-catalyzed oxidant with the chemical signature of ozone showed bactericidal activity in human neutrophils.

What is the biological importance of ozone generated by neutrophils in host defense? MPO catalyzes the reaction to produce hypochlorous acid (HOCl) from hydrogen peroxide (H<sub>2</sub>O<sub>2</sub>) and chloride ion (Cl<sup>-</sup>) (16). MPO deficiency is the most common congenital neutrophil defect. Despite the important role for HOCl in killing microorganisms, MPO-deficient individuals are usually healthy, in sharp contrast to CGD patients (17, 18). However, some MPO-deficient patients revealed an increased susceptibility to infections with bacteria and fungi, particularly those caused by *Candida albicans* (17, 19, 20). In agreement with these facts, MPO-deficient mutant mice, which failed to produce HOCl and subsequent singlet oxygen, showed

an increased susceptibility to pneumonia and death when challenged by high doses of bacteria and fungi, although they were generally healthy under normal conditions (21, 22). In human neutrophils we examined, the bactericidal activity induced by the addition of amino acids was prominent when larger numbers of *E. coli* were added to neutrophils (*E. coli*/neutrophils = 5:1 or 10:1), reminiscent of the MPO deficiency. Thus, ozone produced by neutrophils might potentiate a host defense system when the host is challenged by high doses of infectious agents.

Our current study further suggests the potential therapeutic role for amino acid-catalyzed oxidant with the chemical signature of ozone in infectious diseases. ROS have been playing a central role in photodynamic therapy (PDT) for cancer (23), where light and certain chemicals (photosensitizer) are used. The photosensitizer transfers energy from light to molecular oxygen to generate free radicals/radical ions or singlet oxygen. The ROS that are generated by PDT can kill tumor cells directly, damage the tumor-associated vasculature, and activate an immune response against tumor cells. PDT is now being applied to the treatment of many other diseases, including targeting of microorganisms (24). With an increase in antibiotic resistance, the development of new antimicrobial strategies is expected. In our distinct cell-free system, unexpectedly, the use of a potential photosensitizer, 6FP-tBu-DMF, and UVA, which produced singlet oxygen that is toxic, failed to kill bacteria (Fig. 3A). However, the addition of Trp or Met to 6FP-tBu-DMF and UVA, which produced an oxidant with the chemical signature of ozone, dramatically reduced the rate of viable bacteria (Fig. 3A). These results suggest that our study may contribute to the improvement of antimicrobial PDT.

## Materials and Methods

**Reagents.** Edaravone, human IgG, and human F(ab)<sub>2</sub> were kind gifts from Mitsubishi Pharma. 6FP was obtained from Sankyo Kasei Kogyo. 6FP-tBu-DMF was synthesized in our laboratories at the Institute of Advanced Energy, Kyoto University (9). CLA was purchased from Tokyo Kasei Kogyo; MVP, DHR, and the Amplex Red H<sub>2</sub>O<sub>2</sub> kit were from Molecular Probes. Indigo carmine, gelatin, BSA, dextran, trisodium citrate dihydrate, acetonitrile, and sodium azide were from Nakalai; water-soluble amino acids were from Wako; heart infusion agar was from Nissui; Percoll was from GE Healthcare; zVAD-fmk was from the Peptide Institute; and H<sub>2</sub><sup>18</sup>O (> 97% H<sub>2</sub>O) was from Cambridge Isotope Laboratories. Other chemicals, such as zymosan, FMLP, PMA, SOD, DPI, ABAH, catalase, tetrabutylammoniumhydrogen sulfate (TBA), isatin sulfonic acid, vinylbenzoic acid, and 4-carboxybenzaldehyde, were purchased from Sigma-Aldrich.

**Human CGD Patient.** The human CGD patient was a 25-year-old male with gp91-phox deficiency. Mutation analysis revealed a G-to-A point mutation at nucleotide 252 in exon 3, which produces an aberrant splicing site (25).

**Preparation of Neutrophils.** Human neutrophils were isolated from peripheral blood of healthy adult volunteers and the CGD patient by sedimentation through 2-step Percoll gradients, as described (26). Healthy volunteers and the patient provided written informed consent for participation in an institutional review board-approved protocol at Kyoto University Hospital.

**Ozone Production in the Cell-Free System.** A solution of indigo carmine (30 μM) and 6FP (40 μM) was irradiated for 4 min at 5 mW/cm<sup>2</sup> by using a UVA radiation apparatus (XX-15BLB 625 nm; UVP) in the presence or absence of human immunoglobulins [IgG and F(ab)<sub>2</sub>] (5 mg/mL), BSA (5 mg/mL), FMLP (100 μM), zVAD-fmk (100 μM), or 19 water-soluble amino acids (1 mM) except for tyrosine. In this reaction, indigo carmine was converted to isatin sulfonic acid by ozone. Loss of indigo carmine was monitored by measuring its absorbance at 610 nm with a spectrometer (DU800; Beckman Coulter). For the dose-response reaction, increasing concentrations of Trp, Met, Cys, or His (1 μM to 2 mM) were added to the reaction in the presence of 6FP. Sodium azide (1 mM), edaravone (40 μM), and catalase (2,000 units/mL) were added to the reaction in the presence of 6FP to examine the effects on ozone production by IgG (5 mg/mL), Trp, Met, Cys, and His (1 mM). As a control, a sample without amino acids was analyzed. For HPLC analysis, indigo carmine (100 μM) or vinylbenzoic acid (30 μM) was mixed with 6FP (40 μM) and Met (1 mM) with

or without UVA irradiation for 4 min. The samples were subjected to HPLC analysis.

**HPLC Analysis for the Detection of Isatin Sulfonic Acid and 4-Carboxybenzaldehyde.** The conversion of indigo carmine to isatin sulfonic acid and the oxidation of vinylbenzoic acid to 4-carboxybenzaldehyde were considered as evidence of ozone formation (6). Samples were analyzed on a reverse-phase C<sub>18</sub> HPLC column eluting with 70% 50 mM phosphate buffer (pH 7.2) containing 10 mM TBA and 30% acetonitrile with an L6000 Hitachi HPLC system (indigo carmine, *R*<sub>T</sub> = 12.0 min; isatin sulfonic acid, *R*<sub>T</sub> = 5.1 min; vinylbenzoic acid, *R*<sub>T</sub> = 15.3 min; 4-carboxybenzaldehyde, *R*<sub>T</sub> = 6.4 min) (3, 5). Peak areas were converted to concentrations by comparison to standard curves.

**Assay for Measuring <sup>18</sup>O Isotope Incorporation into Isatin Sulfonic Acid During Indigo Carmine Oxidation by Amino Acid-Catalyzed Water Oxidation.** An aliquot of indigo carmine (150 μM) in phosphate buffer (50 mM, pH 7.4) containing H<sub>2</sub><sup>18</sup>O (> 97% H<sub>2</sub>O) was added to a solution of 6FP (40 μM) in the presence or absence of Met (600 μM) in phosphate buffer (50 mM, pH 7.4) containing H<sub>2</sub><sup>18</sup>O (> 97% H<sub>2</sub>O). The solution was irradiated for 4 min at 5 mW/cm<sup>2</sup> by using an UVA radiation apparatus. Production of isatin sulfonic acid was determined by LC to confirm that reaction had been successful before mass spectral analysis. LC conditions were a reverse-phase C<sub>18</sub> HPLC column and acetonitrile/water (10 mM ammonium acetate) (20:80) mobile phase at 1 mL/min (isatin sulfonic acid, *R*<sub>T</sub> = 2.1 min). MS was measured by using negative ion electrospray MS on a Waters Quattro micro API mass spectrometer. The raw data were extracted into Waters MassLynx version 4.0 format for presentation.

**Bactericidal Assay in the Cell-Free System.** *E. coli* NIHJ-JC2 (5 × 10<sup>6</sup>/mL) were incubated with or without 6FP-tBu-DMF (40 μM) and amino acids (Trp, Met, Arg, or Phe) (1 mM) under UVA irradiation (5 mW/cm<sup>2</sup>) for 2 h. Samples were removed at 60 and 120 min and suspended in water. An aliquot of the suspension was plated on a pour plate made with heart infusion agar. After a 24-h incubation at 37 °C, the colonies formed were counted.

**H<sub>2</sub>O<sub>2</sub> Production in the Cell-Free System and Human Neutrophils.** H<sub>2</sub>O<sub>2</sub> production was measured by using a H<sub>2</sub>O<sub>2</sub> probe, *N*-acetyl-3,7-dihydroxyphenoxazine (Amplex Red), including horseradish peroxidase (27). A solution of 6FP-tBu-DMF (40 μM) and Trp (1 mM), or PMA (50 ng/ml)-stimulated neutrophils (5 × 10<sup>6</sup> cells), were incubated with 50 μM Amplex Red for 2 h at 37 °C. Fluorescence was measured by a fluorometric microplate reader (Fluoroskan Ascent; Labsystems) with excitation and emission wavelengths of 544 and 590 nm, respectively. The amount of H<sub>2</sub>O<sub>2</sub> production was calculated according to the standard curve of H<sub>2</sub>O<sub>2</sub>. To confirm the specificity of this assay, catalase (2,000 units/mL) was added to the reaction before incubation with Amplex Red.

**Bactericidal Effect of H<sub>2</sub>O<sub>2</sub>.** *E. coli* (5 × 10<sup>6</sup>/mL) was incubated with increasing concentrations of H<sub>2</sub>O<sub>2</sub> (0–10<sup>3</sup> mM) for 2 h. Samples were removed at 2 h, and the bactericidal assay was performed as described above.

**Superoxide Release from Neutrophils.** Superoxide production was assessed by the SOD-inhibitable reduction of ferricytochrome *c* as described (28).

**Flow Cytometric DHR Assay.** Neutrophils (5 × 10<sup>5</sup> cells) were loaded with 2 μM DHR for 5 min at 37 °C. After that, the cells were stimulated with 50 ng/ml PMA for 15 min at 37 °C and analyzed by flow cytometry. As a negative control, the pretreatment of neutrophils from a healthy control with 10 μM DPI, an inhibitor of NADPH oxidase, was performed before DHR loading.

**Chemiluminescence Assay.** The productions of superoxide and singlet oxygen of neutrophils stimulated with PMA were examined by using chemiluminescence with an O<sub>2</sub><sup>-</sup>-specific probe, CLA, and an <sup>1</sup>O<sub>2</sub>-specific probe, MVP, respectively. After mixing the neutrophils (2 × 10<sup>6</sup> cells) with 2.5 μM CLA or 40 μM MVP, the mixture was mounted on a luminescence reader (Aloka BLR-301), and the luminescence was monitored every 30 s for 30 min. As a negative control, the pretreatment of neutrophils from a healthy control with 10 μM DPI or 100 μM ABAH, an inhibitor of MPO, was performed.

**Ozone Production of CGD Neutrophils.** Indigo carmine (30 μM) was incubated with unstimulated or PMA (50 ng/ml)-stimulated CGD neutrophils (1 × 10<sup>6</sup>/mL) in the presence or absence of 1 mM Trp for 2 h at 37 °C. Edaravone (40 μM) was added to the reaction to examine the effect on ozone production. The loss of indigo carmine was monitored as described above. Vinylbenzoic acid (100 μM) was incubated with unstimulated or PMA (50 ng/ml)-stimulated CGD

neutrophils ( $1 \times 10^6/\text{mL}$ ) in the presence or absence of 1 mM Trp for 2 h at 37 °C. The samples were subjected to HPLC analysis as described above.

**Bactericidal Assay of Human Neutrophils.** Bactericidal activity of human neutrophils was determined by a standard technique (29). Briefly, the reaction mixture contained  $2.5 \times 10^6$  neutrophils,  $2.5 \times 10^6$  (PMN:*E. coli* = 1:1), or  $1.25 \times 10^7$  (1:5), or  $2.5 \times 10^7$  (1:10) *E. coli* cells, 10% human AB serum, 0.1% gelatin, and HBSS. The mixture was incubated with or without 1 mM Trp at

37 °C. Samples were removed at 60 and 120 min, and the bactericidal assay was performed as described above.

**Statistical Analysis.** Data are expressed as the mean  $\pm$  SD.  $P < 0.05$  by the paired Student's *t* test was considered significant.

**ACKNOWLEDGMENTS.** We thank Dr. Hiroyuki Nunoi for genetic analysis of the CGD patient and Dr. Harry L Malech for helpful discussions. This work was supported by the Mitsubishi Pharma Foundation.

- Williams R (2006) Killing controversy. *J Exp Med* 203:2404.
- Wentworth P, Jr, et al. (2002) Evidence for antibody-catalyzed ozone formation in bacterial killing and inflammation. *Science* 298:2195–2199.
- Babior BM, Takeuchi C, Ruedi J, Gutierrez A, Wentworth P, Jr (2003) Investigating antibody-catalyzed ozone generation by human neutrophils. *Proc Natl Acad Sci USA* 100:3031–3034.
- Nieva J, Wentworth P, Jr (2004) The antibody-catalyzed water oxidation pathway: A new chemical arm to immune defense? *Trends Biochem Sci* 29:274–278.
- Kettle AJ, Clark BM, Winterbourn CC (2004) Superoxide converts indigo carmine to isatin sulfonic acid: Implications for the hypothesis that neutrophils produce ozone. *J Biol Chem* 279:18521–18525.
- Kettle AJ, Winterbourn CC (2005) Do neutrophils produce ozone? An appraisal of current evidence. *Biofactors* 24:41–45.
- Malech HL (1993) Phagocyte oxidative mechanisms. *Curr Opin Hematol* 1:123–132.
- Weening RS, Adriaansz LH, Weemaes CM, Lutter R, Roos D (1985) Clinical differences in chronic granulomatous disease in patients with cytochrome *b*-negative or cytochrome *b*-positive neutrophils. *J Pediatr* 107:102–104.
- Yamada H, et al. (2005) Photodynamic effects of a novel pterin derivative on a pancreatic cancer cell line. *Biochem Biophys Res Commun* 333:763–767.
- Sommani P, et al. (2007) Effects of edaravone on singlet oxygen released from activated human neutrophils. *J Pharmacol Sci* 103:117–120.
- Vowells SJ, et al. (1996) Genotype-dependent variability in flow cytometric evaluation of reduced nicotinamide adenine dinucleotide phosphate oxidase function in patients with chronic granulomatous disease. *J Pediatr* 128:104–107.
- Nakano M, Sugioka K, Ushijima Y, Goto T (1986) Chemiluminescence probe with cypridina luciferin analog, 2-methyl-6-phenyl-3,7-dihydroimidazo[1,2-*a*]pyrazin-3-one, for estimating the ability of human granulocytes to generate  $\text{O}_2^-$ . *Anal Biochem* 159:363–369.
- Posner GH, et al. (1984) A chemiluminescent probe specific for singlet oxygen. *Biochem Biophys Res Commun* 123:869–873.
- Teixeira MM, Cunha FQ, Noronha-Dutra A, Hothersall J (1999) Production of singlet oxygen by eosinophils activated in vitro by C5a and leukotriene B4. *FEBS Lett* 453:265–268.
- Yamashita K, et al. (2001) 6-Formylpterin intracellularly generates hydrogen peroxide and restores the impaired bactericidal activity of human neutrophils. *Biochem Biophys Res Commun* 289:85–90.
- Klebanoff SJ (2005) Myeloperoxidase: Friend and foe. *J Leukocyte Biol* 77:598–625.
- Parry MF, et al. (1981) Myeloperoxidase deficiency: Prevalence and clinical significance. *Ann Intern Med* 95:293–301.
- Suzuki K, Muso E, Nauseef WM (2004) Contribution of peroxidases in host-defense, diseases, and cellular functions. *Jpn J Infect Dis* 57:S1–S2.
- Lehrer RI, Cline MJ (1969) Leukocyte myeloperoxidase deficiency and disseminated candidiasis: The role of myeloperoxidase in resistance to *Candida* infection. *J Clin Invest* 48:1478–1488.
- Nguyen C, Katner HP (1997) Myeloperoxidase deficiency manifesting as pustular candida dermatitis. *Clin Infect Dis* 24:258–260.
- Aratani Y, et al. (1999) Severe impairment in early host defense against *Candida albicans* in mice deficient in myeloperoxidase. *Infect Immun* 67:1828–1836.
- Aratani Y, et al. (2000) Differential host susceptibility to pulmonary infections with bacteria and fungi in mice deficient in myeloperoxidase. *J Infect Dis* 182:1276–1279.
- Dolmans DE, Fukumura D, Jain RK (2003) Photodynamic therapy for cancer. *Nat Rev Cancer* 3:380–387.
- Maisch T (2007) Antimicrobial photodynamic therapy: Useful in the future? *Lasers Med Sci* 22:83–91.
- Roos D, et al. (1996) Mutations in the X-linked and autosomal recessive forms of chronic granulomatous disease. *Blood* 87:1663–1681.
- Moriguchi T, et al. (1990) Studies of the functions of polymorphonuclear leukocytes obtained from human bone marrow. *Acta Hematol Jpn* 53:668–677.
- Zhou M, Panchuk-Voloshina N (1997) A 1-step fluorometric method for the continuous measurement of monoamine oxidase activity. *Anal Biochem* 253:169–174.
- Asagoe K, et al. (1998) Down-regulation of CXCR2 expression on human polymorphonuclear leukocytes by TNF- $\alpha$ . *J Immunol* 160:4518–4525.
- Johnston RB, Jr, et al. (1975) The role of superoxide anion generation in phagocytic bactericidal activity. Studies with normal and chronic granulomatous disease leukocytes. *J Clin Invest* 55:1357–1372.

ORIGINAL ARTICLE: RESEARCH

## Abnormal cytoplasmic dyslocalisation and/or reduction of nucleophosmin protein level rarely occurs in myelodysplastic syndromes

YUICHI ISHIKAWA<sup>1\*</sup>, JINGLAN XU<sup>1\*</sup>, GYOSUKE SAKASHITA<sup>2</sup>, TAKESHI URANO<sup>2</sup>, TATSUYA SUZUKI<sup>1</sup>, AKIHIRO TOMITA<sup>1</sup>, HITOSHI KIYOI<sup>3</sup>, SHIGEO NAKAMURA<sup>4</sup>, & TOMOKI NAOE<sup>1</sup>

<sup>1</sup>Department of Hematology and Oncology, Nagoya University Graduate School of Medicine, Showa-ku, Nagoya, Japan, <sup>2</sup>Department of Biochemistry, Shimane University School of Medicine, Izumo, Japan, <sup>3</sup>Department of Infectious Diseases, Nagoya University Hospital, Showa-ku, Nagoya, Japan, and <sup>4</sup>Department of Pathophysiology, Nagoya University Hospital, Showa-ku, Nagoya, Japan

(Received 6 September 2008; accepted 8 October 2008)

### Abstract

The Nucleophosmin1 (*NPM1*) gene located in chromosome 5q35 is affected by chromosomal translocation, mutation and deletion in myelodysplastic syndrome (MDS) and acute myeloid leukemia (AML). *NPM1* haploinsufficiency reportedly causes MDS-like disorders in knockout mice. Here, we studied mRNA and protein expression in bone marrow (BM) samples from 36 patients with MDS. The *NPM1* expression levels of mRNA and protein were not related to chromosome 5 abnormalities and were almost the same as those in normal BM and AML cells. However, the protein levels in AML cells with *NPM1* mutations were slightly lower than in those without mutation. Immunohistochemical studies showed no difference in the staining intensity and subcellular localisation between MDS and normal BM cells. It was concluded that abnormal cytoplasmic localisation and/or significant reduction of *NPM1* protein level rarely occurs in MDS. The increase in the number of nuclear *NPM1*-positive cells may be related to the progression of MDS.

**Keywords:** Nucleophosmin, myelodysplastic syndrome, immunohistochemical staining

### Introduction

Nucleophosmin1 (*NPM1*) is a nucleolar phosphoprotein with multiple biological roles [1–5]. In hematological malignancies, the *NPM1* is affected by chromosomal translocation, mutation and deletion [6–8]. The *NPM1* on 5q35 is translocated with the *ALK* in anaplastic large cell lymphoma with t(2;5) [9]. The *MLF1* and *RARA* genes are fused with *NPM1* in myelodysplastic syndrome (MDS)/acute myeloid leukemia (AML) with t(3;5) [10] and acute promyelocytic leukemia with t(5;17) [11], respectively. Most importantly, mutations in exon 12 have been found in a significant proportion of *de novo* AML cases, especially in those with a normal karyotype [12–16]. Mutant *NPM* is aberrantly

localised in the cytoplasm, but the molecular mechanisms associated with leukemia remain unclear. The knockout mice model of the *NPM1* gene suggests that *NPM1*<sup>+/-</sup> haploinsufficiency causes hematological disorders like MDS [17]. Because the *NPM1* gene locus on 5q35 is often deleted in MDS and AML, loss-of-heterozygosity and/or mutation have been studied in human MDS samples [18]. According to previous reports, however, mutation of the *NPM1* exon 12 is very rare in MDS either in combination with 5q abnormality or not. Furthermore, the promoter region of *NPM1* is rarely methylated [19], suggesting that *NPM1* may not simply have a role as a tumor suppressor gene in MDS. To further clarify the involvement of *NPM1* in MDS, we generated a new antibody to *NPM* and

Correspondence: Yuichi Ishikawa, Department of Hematology and Oncology, Nagoya University Graduate School of Medicine, 65 Tsurumai-cho, Showa-ku, Nagoya 466-8560, Japan. Tel: +81-52-744-2955. Fax: +81-52-744-2801. E-mail: yishikaw@med.nagoya-u.ac.jp  
\*These authors equally contributed to this work.

analysed the expression levels and subcellular localisation of NPM in MDS.

## Materials and methods

### Patient samples

*NPM1* expression and mutation were analysed in bone marrow (BM) cells and specimens from 36 patients with newly diagnosed MDS at the Nagoya University Hospital. Diagnosis was made according to the FAB classification. MDS patients consisted of 24 men and 12 women with a median age of 58 years (range, 28–89 years). Four secondary AML patients with MDS were also studied. BM mononuclear cells were harvested by standard Ficoll/Paque density gradient centrifugation (Amersham Pharmacia Biosciences, Roosendaal, The Netherlands) and were suspended in RPMI1640 medium supplemented with 10% fetal bovine serum, 100 IU/mL of penicillin G and 100 µg/mL of streptomycin. Informed consent was obtained from all patients to use their samples for banking and molecular analysis, and approval was obtained from the ethical committee of Nagoya University School of Medicine for these studies.

### Antibodies

Anti-NPM mouse monoclonal antibody (NPM9.2.6) specific for bacterially expressed NPM1 was generated, then, purified from BL21 transformed with pGEX 4T-2 carrying full-length human NPM1. To determine the epitope of this antibody, HeLa cells were transfected for 48 h with human NPM1, NPM1.2 and their truncated mutants were tagged with EGFP. Cells were then lysed with SDS-sample buffer followed by sonication. Western blot analysis was performed with anti-NPM 9.2.6 and anti-EGFP rabbit polyclonal antibody (MBL). To characterise the cross-reactivity between species, lysates were prepared from HeLa and NIH3T3 cells. Western blot analysis was performed with anti-NPM 9.2.6, anti-B23 mouse monoclonal antibody (B0556, Sigma) and anti- $\alpha$ -tubulin mouse monoclonal antibody (T6199, Sigma).

### Characterisation of anti NPM 9.2.6 monoclonal antibody

Anti-NPM mouse monoclonal antibody 9.2.6 can recognise both human NPM1 and NPM1.2, the epitope of which is located in the region of 170–189 aa (Supplement Figure 1A). However, this antibody cannot recognise mouse NPM (Supplement Figure 1B, upper panel) despite the expression level

being comparable between the cell lines (Supplement Figure 1B, middle panel).

### Real time quantitative PCR

Total RNA was extracted from the samples by using a QIAamp RNA Blood Mini Kit (Qiagen, Chatsworth, CA). cDNA was synthesised from each RNA using a random primer and Moloney murine leukemia virus reverse transcriptase (SuperScript II; Invitrogen) according to the manufacturer's recommendations. The expression level of NPM1 transcripts were quantified using a real-time fluorescence detection method on an ABI prism7000 sequence detection system following the manufacturer's recommendations (Applied Biosystem, Foster City, CA). PCR procedures were carried out at 50°C for 2 min, 95°C for 10 min, followed by 40 PCR cycles at 95°C for 15 s and 60°C for 1 min. The housekeeping gene, GAPDH, served as a control for cDNA quality. Each gene expression level was analysed in duplicate and the expression level was calculated as previously described [20].

### Screening for mutation of the NPM1 gene

For the screening of *NPM1* mutations, we amplified genomic DNA corresponding to exon 12 of *NPM1* by PCR using the primers NPM1-F, 5'-TTAACTCTCTGGTGGTGTAGAATGAA-3' and NPM1-R, 5'-CAAGACTATTTGCCATTCC TAAC-3', as previously reported [6]. Amplified products were separated through agarose gel, purified using a QIAquick gel extraction kit (Qiagen) and directly sequenced on a DNA sequencer (310; Applied Biosystems) using a BigDye terminator cycle sequencing kit (Applied Biosystems). If mutations were found by direct sequencing, the fragments were cloned into a pGEM-T Easy vector (Promega, Madison, WI), then transfected into *Escherichia coli* strain DH5 $\alpha$ . At least four recombinant colonies were selected and plasmid DNA was prepared using a QIAprep Spin Miniprep Kit (Qiagen) and sequenced.

### Immunohistochemical staining

Samples were fixed with ice-cold 4% paraformaldehyde for 16–24 h, embedded in paraffin, sectioned transversely (thickness, 3 µm) and processed so that immunohistochemical techniques could be used to determine the localisation of NPM. After removal of paraffin with xylene and dehydration with a series of ethanol solutions, the tissue sections were subjected to microwave irradiation (750 W) for 15 min in 0.01 mol/L citrate buffer (pH 6.0). The sections were then placed in

an automated immunostainer (Ventana Medical Systems, Tucson, AZ) as described [21]. For negative controls, primary antibodies were replaced with mouse IgG. We investigated a single case twice for NPM expression. The entire section was screened to find the region with the highest immunostaining.

**Immunoblotting**

A total of  $1-5 \times 10^6$  fresh or frozen cells were directly lysed in sample buffer and then subjected to SDS-polyacrylamide gel electrophoresis on a 10% gel and the separated proteins were then transferred to a polyvinylidene difluoride membrane (Millipore Corp., Bedford, MA, USA). The membrane was incubated at room temperature first for 1 h with 5% non-fat milk and 0.1% Tween-20 in Tris-buffered saline and then kept overnight with the appropriately diluted mouse monoclonal antibodies in the same solution. After washing, the membrane was incubated for 1 h with diluted horseradish peroxidase-conjugated mouse antibody to mouse IgG (MBL) and immune complexes were then detected with ECL reagents (Amersham).

**Results**

The expression level of the *NPM1* transcripts in MDS cells was studied and compared with those in normal and AML cells (Figure 1). In normal peripheral blood, the median expression level of the *NPM1* transcripts was  $8.0$  (range,  $3.2-9.5$ )  $\times 10^6$ ,  $9.4$

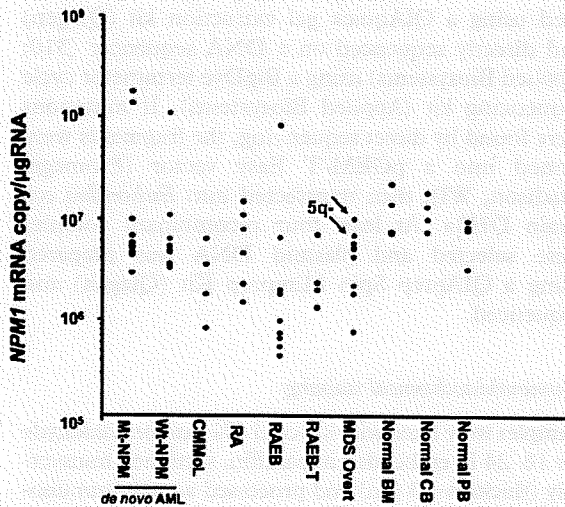


Figure 1. Real-time quantitative PCR of *NPM1* transcripts. Distribution of the expression level of the *NPM1* mRNA in AML, MDS and normal samples are indicated, the arrowed dots indicate that the patients carrying a 5q- abnormality. There were no significant differences in the sequence of exon12 of *NPM1*, the FAB type and normal samples.

(range,  $1.6-12$ )  $\times 10^6$ ,  $10.8$  ( $7.2-22$ )  $\times 10^6$  copies/ $\mu$ g RNA in normal peripheral blood cells, cord blood cells and BM cells, respectively. The median expression levels in MDS cells was  $2.0$  (range,  $0.2-83$ )  $\times 10^6$  copies/ $\mu$ g RNA, which was a lower level than that those of normal cells, but the expression levels of *NPM1* transcripts were not statistically different between MDS samples and normal BM samples ( $p=0.163$ , by Mann-Whitney test). In two patients with secondary AML carrying a 5q abnormality, the mRNA level was not lower. Mutations in exon 12 of the *NPM1* gene were analysed in 36 patients with RA, RAEB and RAEB-T. In two (5%) patients with RAEB, 4-bp was inserted into the common site of exon 12, and mRNA levels in both cases were the same as for those without the mutation.

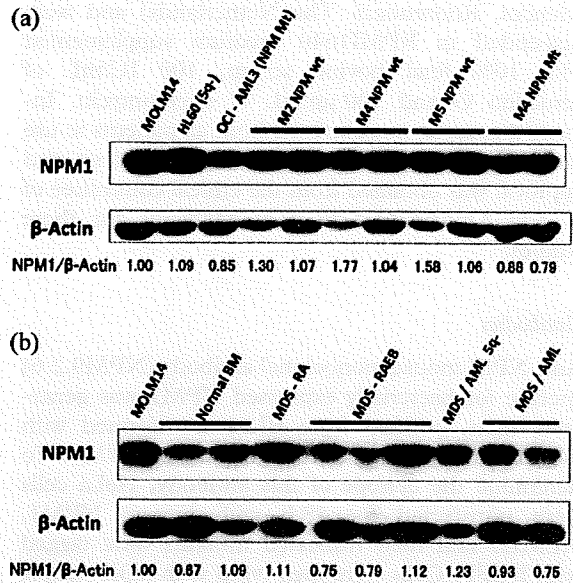


Figure 2. *NPM1* protein detected by immunoblotting. The expression level of *NPM1* protein in clinical samples and cell lines was analysed by immunoblotting. Protein signal intensities were measured and normalised with the signal intensities of  $\beta$ -actin. The normalised *NPM1*  $\beta$ -actin ratio is indicated below, the ratio of MOLM14 cell is used as a control. (A) In AML cell line, the expression level of *NPM1* in HL60 cell carrying 5q deletion was almost equally to that of MOLM14 cell carrying intact chromosome 5, each cell lines possessed wild-type *NPM1*. Although in OCI-AML3 cell carrying *NPM1* mutation, the slightly lower expression of *NPM1* protein level was observed. In AML samples, immunoblotting analysis of M2, M4 with and M5 according to FAB classification samples with wild-type *NPM1* revealed that the expression level of *NPM1* protein was almost at the same level as the FAB type. In AML samples with mutated *NPM1*, the expression level of *NPM1* protein was slightly lower than that in AML cells without *NPM1* mutation, in spite of the same FAB type. (B) The expression level of *NPM1* protein was compared in MDS samples according to FAB type and normal bone marrow mononuclear cells. There was no significance in the difference in expression level of *NPM1* protein between MDS samples with or without 5q- and normal BM samples.

To study the levels of NPM1 protein expression, a total of 21 samples from healthy volunteers, AML patients and MDS patients were subjected to immunoblot analysis. Anti-NPM antibody (9.2.6)

detected bands at a molecular weight of 37 kDa, corresponding to NPM, in all samples. The NPM level in AML cells with *NPM1* mutation was slightly lower than that in AML cells without *NPM1*

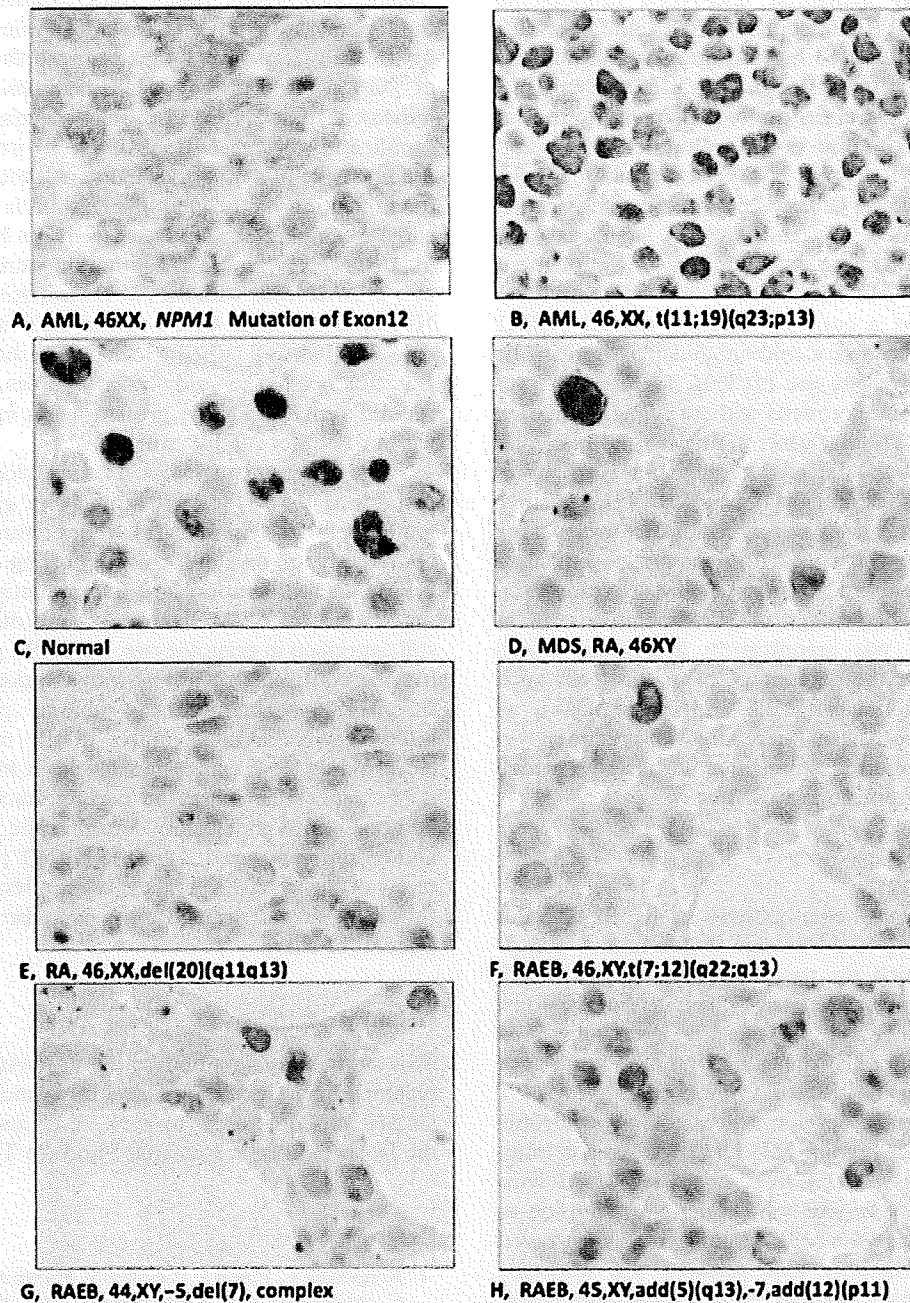


Figure 3. Immunohistochemistry of NPM1. The immunohistochemical studies of the NPM1 in AML, MDS and normal samples are indicated with karyotype. (A) In AML with *NPM1* mutation, NPM was diffusely stained in a microgranular pattern in the cytoplasm as well as the nucleus, as reported previously. (B) In AML without *NPM1* mutation, nuclear and nucleolar staining was clearly detected in leukemia cells. (C) In Normal BM cells, nuclear and nucleolar staining was detected in a part of lymphoid and myeloid cells. (D-H) In MDS, positive nuclear staining was observed in relatively large myeloid cells, which was similar to the staining pattern in normal BM.



mutation (mean relative intensity: 0.85 vs. 1.08,  $p=0.01$ , Figure 2A). In MDS, the expression levels varied among samples but the expression level was similar to that of AML cells without *NPM1* mutation (0.93 vs. 1.08,  $p=0.13$ , Figure 2A). No aberrant bands were detected in these samples (Figure 2B).

Using newly generated anti-NPM monoclonal antibody (NPM 9.2.6), both NPM1.1 and NPM1.2 proteins were detected by immunoblot analysis and immunohistochemical techniques. In normal BM cells, NPM1 was clearly detected in mononuclear myeloid cells but not in polymorphonuclear cells and erythroblasts. Lack of NPM1 expression in the polymorphonuclear cells was confirmed using normal peripheral blood by immunoblot analysis and immunohistochemical techniques (Supplement Figure 2). In AML specimens with *NPM1* mutation (Figure 3A) as a control, diffusely stained NPM1 could be observed as a microgranular pattern in the cytoplasm as well as the nucleus, as reported previously. In AML specimens without *NPM1* mutation (Figure 3B) as another control, nuclear and nucleolar staining was clearly detected in leukemia cells.

In MDS specimens (Figure 3D–H), positive nuclear staining was observed in relatively large myeloid cells, which was fundamentally similar to the staining pattern in normal BM (Figure 3C). However, the percentage of NPM-positive cells in the specimen was significantly decreased, which is explained by the percentage of mature cells such as polymorphonuclear cells and lymphocytes, as well as erythroblasts. There are no specimens in which NPM showed subcellular localisation which was different from normal BM cells.

## Discussion

MDS is a clonal hematopoietic stem cell disorder characterised by multi-lineage dysplasia and pancytopenia in which the molecular mechanism is still mainly unclear, and even that which is understood is, quite heterogeneous [22]. Recently, it was suggested that *NPM1* might play the role of a tumor-suppressor gene in MDS in light of findings that *NPM1*<sup>+/-</sup> heterozygous mice develop a hematologic syndrome with features of human MDS [17]. During a long-time observation, *NPM1*<sup>+/-</sup> mice developed lymphoid malignancies and solid tumors, in addition to myeloid malignancies [23]. Malignant cells displayed multiple centrosomes and retained the wild-type allele and NPM1 protein with normal subcellular localisation and expression level. If this haploinsufficiency model is applicable to human MDS, the expression level of NPM1 must be critical for development or suppression of MDS. According to Knudson's two-hit model, two successive events,

such as a deletion, mutation or methylation, in both alleles of a tumor-suppressor gene are required to turn a normal cell into a cancer cell [23]. In this case, the tumor-suppressor protein almost loses its function entirely. Because NPM1 has a critical role in ribosome biogenesis and cell proliferation, a haploinsufficiency model rather than Knudson's two-hit model may fit better with the above mice model. So far no study has carefully investigated the expression of NPM1 in human MDS samples. Here, we indicated that NPM1 protein levels were not significantly decreased in MDS cells irrespective of the presence of a 5q abnormality. Although accurate quantification of protein expression is difficult in clinical samples, our study showed that NPM1 levels in AML cells with *NPM1* mutation were lower than that in AML cells without *NPM1* mutation. Mutated NPM protein might have a shorter half-life than wild-type NPM as well as being localised in the cytoplasm. But, it is needed to study more samples to elucidate the differences of NPM protein levels in AML cells with or without *NPM1* mutation.

The immunohistochemical study clearly showed that NPM was expressed scarcely in granulocytes, moderately in lymphocytes and erythroblasts and abundantly in myeloblasts, supporting the role of NPM1 in proliferation and differentiation. Because the amount of *NPM1* transcripts are decreased but still expressed in granulocytes, the NPM protein level may be controlled by a post-transcriptional manner. In MDS specimens, the staining pattern and intensity were almost similar to the normal BM. Accordingly, low expression levels in immunoblots might reflect the increased mature fractions in the BM cells. In conclusion, cytoplasmic localisation and/or significant reduction of NPM1 protein level rarely occur in MDS. The expression level of NPM1 should be further studied in the stem/progenitor cell fraction of MDS.

## Acknowledgments

This study was supported by Grant-in-Aids from the National Institute of Biomedical Innovation (to T.N.), for Scientific Research (to T.N., T.U. and G.S.) and the Japan Leukemia Research Fund (to T.U.).

## References

1. Korgaonkar C, Hagen J, Tompkins V, Frazier AA, Allamargot C, Quelle FW, et al. Nucleophosmin (B23) targets ARF to nucleoli and inhibits its function. *Mol Cell Biol* 2005;25:1258–1271.
2. Kurki S, Peltonen K, Latonen L, Kiviharju TM, Ojala PM, Meek D, et al. Nucleolar protein NPM interacts with HDM2 and protects tumor suppressor protein p53 from HDM2-mediated degradation. *Cancer Cell* 2004;5:465–475.

3. Colombo E, Marine JC, Danovi D, Falini B, Pelicci PG. Nucleophosmin regulates the stability and transcriptional activity of p53. *Nat Cell Biol* 2002;4:529-533.
4. Borer RA, Lehner CF, Eppenberger HM, Nigg EA. Major nucleolar proteins shuttle between nucleus and cytoplasm. *Cell* 1989;56:379-390.
5. Chan WY, Liu QR, Borjigin J, Busch H, Rennert OM, Tease LA, et al. Characterization of the cDNA encoding human nucleophosmin and studies of its role in normal and abnormal growth. *Biochemistry* 1989;28:1033-1039.
6. Falini B, Mecucci C, Tiacci E, Alcalay M, Rosati R, Pasqualucci L, et al. Cytoplasmic nucleophosmin in acute myelogenous leukemia with a normal karyotype. *N Engl J Med* 2005;352:254-266.
7. Grisendi S, Mecucci C, Falini B, Pandolfi PP. Nucleophosmin and cancer. *Nat Rev Cancer* 2006;6:493-505.
8. Naoe T, Suzuki T, Kiyoi H, Urano T. Nucleophosmin: a versatile molecule associated with hematological malignancies. *Cancer Sci* 2006;97:963-969.
9. Morris SW, Kirstein MN, Valentine MB, Dittmer K, Shapiro DN, Look AT, et al. Fusion of a kinase gene, ALK, to a nucleolar protein gene, NPM, in non-Hodgkin's lymphoma. *Science* 1995;267:316-317.
10. Yoneda-Kato N, Look AT, Kirstein MN, Valentine MB, Raimondi SC, Cohen KJ, et al. The t(3;5)(q25.1;q34) of myelodysplastic syndrome and acute myeloid leukemia produces a novel fusion gene, NPM-MLF1. *Oncogene* 1996;12:265-275.
11. Redner RL, Rush EA, Faas S, Rudert WA, Corey SJ. The t(5;17) variant of acute promyelocytic leukemia expresses a nucleophosmin-retinoic acid receptor fusion. *Blood* 1996;87:882-886.
12. Thiede C, Koch S, Creutzig E, Steudel C, Illmer T, Schaich M, et al. Prevalence and prognostic impact of NPM1 mutations in 1485 adult patients with acute myeloid leukemia (AML). *Blood* 2006;107:4011-4020.
13. Verhaak RG, Goudswaard CS, van Putten W, Bijl MA, Sanders MA, Hagens W, et al. Mutations in nucleophosmin (NPM1) in acute myeloid leukemia (AML): association with other gene abnormalities and previously established gene expression signatures and their favorable prognostic significance. *Blood* 2005;106:3747-3754.
14. Schnittger S, Schoch C, Kern W, Mecucci C, Tschulik C, Martelli MF, et al. Nucleophosmin gene mutations are predictors of favorable prognosis in acute myelogenous leukemia with a normal karyotype. *Blood* 2005;106:3733-3739.
15. Dohner K, Schlenk RF, Habdank M, Scholl C, Rucker FG, Corbacioglu A, et al. Mutant nucleophosmin (NPM1) predicts favorable prognosis in younger adults with acute myeloid leukemia and normal cytogenetics: interaction with other gene mutations. *Blood* 2005;106:3740-3746.
16. Suzuki T, Kiyoi H, Ozeki K, Tomita A, Yamaji S, Suzuki R, et al. Clinical characteristics and prognostic implications of NPM1 mutations in acute myeloid leukemia. *Blood* 2005;106:2854-2861.
17. Grisendi S, Bernardi R, Rossi M, Cheng K, Khandker L, Manova K, et al. Role of nucleophosmin in embryonic development and tumorigenesis. *Nature* 2005;437:147-153.
18. Berger R, Busson M, Baranger L, Helias C, Lessard M, Dastugue N, et al. Loss of the NPM1 gene in myeloid disorders with chromosome 5 rearrangements. *Leukemia* 2006;20:319-321.
19. Oki Y, Jelinek J, Beran M, Verstovsek S, Kantarjian HM, Issa JP. Mutations and promoter methylation status of NPM1 in myeloproliferative disorders. *Haematologica* 2006;91:1147-1148.
20. Ozeki K, Kiyoi H, Hirose Y, Iwai M, Ninomiya M, Kodera Y, et al. Biologic and clinical significance of the FLT3 transcript level in acute myeloid leukemia. *Blood* 2004;103:1901-1908.
21. Xu JL, Lai R, Kinoshita T, Nakashima N, Nagasaka T. Proliferation, apoptosis, and intratumoral vascularity in multiple myeloma: correlation with the clinical stage and cytological grade. *J Clin Pathol* 2002;55:530-534.
22. Corey SJ, Minden MD, Barber DL, Kantarjian H, Wang JC, Schimmer AD. Myelodysplastic syndromes: the complexity of stem-cell diseases. *Nat Rev Cancer* 2007;7:118-129.
23. Sportoletti P, Grisendi S, Majid SM, Cheng K, Clohessy JG, Viale A, et al. Npm1 is a haploinsufficient suppressor of myeloid and lymphoid malignancies in the mouse. *Blood* 2008;111:3859-3862.

# Acetylation of PML Is Involved in Histone Deacetylase Inhibitor-mediated Apoptosis<sup>\*§</sup>

Received for publication, March 20, 2008, and in revised form, July 7, 2008. Published, JBC Papers in Press, July 11, 2008, DOI 10.1074/jbc.M802217200

Fumihiko Hayakawa<sup>†1</sup>, Akihiro Abe<sup>‡</sup>, Issay Kitabayashi<sup>§5</sup>, Pier Paolo Pandolfi<sup>¶9</sup>, and Tomoki Naoe<sup>‡</sup>

From the <sup>†</sup>Department of Hematology and Oncology, Nagoya University, Graduate School of Medicine, Nagoya 466-8550, Japan, the <sup>§</sup>Molecular Oncology Division, National Cancer Center Research Institute, 5-1-1 Tsukiji, Chuo-ku, Tokyo 104-0045, Japan, and the <sup>¶</sup>Cancer Genetics Program, Beth Israel Deaconess Cancer Center, Department of Medicine, Harvard Medical School, Boston, Massachusetts 02215

PML is a potent tumor suppressor and proapoptotic factor and is functionally regulated by post-translational modifications such as phosphorylation, sumoylation, and ubiquitination. Histone deacetylase (HDAC) inhibitors are a promising class of targeted anticancer agents and induce apoptosis in cancer cells by largely unknown mechanisms. We report here a novel post-transcriptional modification, acetylation, of PML. PML exists as an acetylated protein in HeLa cells, and its acetylation is enhanced by coexpression of p300 or treatment with a HDAC inhibitor, trichostatin A. Increased PML acetylation is associated with increased sumoylation of PML *in vitro* and *in vivo*. PML is involved in trichostatin A-induced apoptosis and PML with an acetylation-defective mutation shows an inability to mediate apoptosis, suggesting the importance of PML acetylation. Our work provides new insights into PML regulation by post-translational modification and new information about the therapeutic mechanism of HDAC inhibitors.

The promyelocytic leukemia protein PML controls cell cycle progression, senescence, and cell death (1, 2). Wild-type PML is a potent growth suppressor that, when overexpressed, can block cell cycle progression in a variety of tumor cell lines (1); conversely PML<sup>-/-</sup> mouse embryo fibroblasts (MEFs)<sup>2</sup> replicate significantly faster than their PML<sup>+/+</sup> MEFs (3). PML also plays an essential role in DNA damage or stress-induced apoptosis, and PML<sup>-/-</sup> cells are resistant to a variety of apoptotic signals (4). In normal cells, the PML protein is localized in, and essential for the biogenesis of, discrete subnuclear compart-

ments designated as nuclear bodies (NBs) (5). In NBs, PML coaccumulates with more than 70 kinds of proteins that are involved in tumor suppression, apoptosis, regulation of gene expression, anti-viral response, and DNA repair. PML is thought to exert its function by regulating the function of binding partners as a core of NBs (6). Intriguingly, NBs are disrupted in human acute promyelocytic leukemia cells by PML-RAR $\alpha$ , an oncogenic fusion protein of PML, and RAR- $\alpha$ , which is thought to be the mechanism of anti-apoptotic effect of PML-RAR $\alpha$  (7–9).

It has been reported that NB formation requires PML to be conjugated to SUMO-1 (5, 10). SUMO-1 is an 11-kDa protein that is structurally homologous to ubiquitin (11). Sumoylation is thought to regulate the subcellular localization, stability, DNA binding, and/or transcriptional ability of its target proteins such as PML, Ran GTPase-activating protein (RanGAP)1, I $\kappa$ B $\alpha$ , and heat shock transcription factor 2 (11). Virtually As<sub>2</sub>O<sub>3</sub>, a chemotherapeutic agent clinically used in the treatment of acute promyelocytic leukemia cells, induces PML sumoylation. Increased PML sumoylation induced by As<sub>2</sub>O<sub>3</sub> treatment leads to the restoration of NBs disrupted by PML-RAR $\alpha$  and then is followed by apoptosis in acute promyelocytic leukemia cells, which results in prolonged remission of the disease (12–15). These findings underscore the importance of PML sumoylation and the integrity of NBs to tumor suppression.

Histone deacetylase (HDAC) inhibitors, a promising class of targeted anticancer agents, can block proliferation and induce cell death in a wide variety of transformed cells (16). HDAC inhibitors block the activity of class I and II HDACs and induce histone acetylation, which leads to the relaxation of chromatin structure, enhanced accessibility of transcription machinery to DNA, and increased gene transcription (17). HDAC inhibitors also induce acetylation of transcription factors, which alters their activities and the expression of their target genes (18). Recent studies demonstrated that p53 acetylation induced by a HDAC inhibitor leads to expression of proapoptotic proteins such as Bax, PIG3, and NOXA (19, 20). However, the mechanisms of p53-independent apoptosis by HDAC inhibitor remain largely unknown.

Here, we report PML acetylation as its novel post-transcriptional modification. PML acetylation is induced by trichostatin A (TSA), a HDAC inhibitor. This enhanced acetylation leads to increased PML sumoylation and may play a key role in TSA-induced apoptosis. This work provides new insights into the

\* This work was supported by grants-in-aid from the Uehara Memorial Foundation, the National Institute of Biomedical Innovation, and the Ministry of Education, Culture, Sports, Science, and Technology of Japan. The costs of publication of this article were defrayed in part by the payment of page charges. This article must therefore be hereby marked "advertisement" in accordance with 18 U.S.C. Section 1734 solely to indicate this fact.

§ The on-line version of this article (available at <http://www.jbc.org>) contains supplemental Fig. S1–S9 and supplemental data.

<sup>1</sup> To whom correspondence should be addressed: Dept. of Hematology and Oncology, Nagoya University, Graduate School of Medicine, 65 Tsurumai-cho, Showa-ku, Nagoya, 466-8550, Japan. Fax: 81-52-744-2161; E-mail: bun-hy@med.nagoya-u.ac.jp.

<sup>2</sup> The abbreviations used are: MEF, mouse embryo fibroblast; HDAC, histone deacetylase; TSA, trichostatin A; NB, nuclear body; RAR, retinoic acid receptor; SUMO, small ubiquitin-like modifier; HAT, histone acetyltransferase; GST, glutathione S-transferase; HA, hemagglutinin; GFP, green fluorescent protein.

functional regulation of PML and the therapeutic mechanisms of treatment with HDAC inhibitors.

## EXPERIMENTAL PROCEDURES

**Antibodies, Plasmids, and Cell Culture**—The sources of antibodies and plasmids and the cell culture conditions are detailed in the supplemental data.

**Transient Transfection, Immunoprecipitation, Immunoblotting, Immunofluorescence, and in Vitro and in Vivo Acetylation Assays**—These were performed as described previously (21, 28) except transient transfections into PML<sup>-/-</sup> MEFs were performed by nucleofection using the Nucleofector system (Amaxa Biosystems) according to the manufacturer's instructions.

**Antibody Array Assay and Detection and Quantification of Apoptosis**—These are also detailed in the supplemental data.

**In Vitro Sumoylation Assay**—The *in vitro* sumoylation assay was performed essentially as described previously (21), except recombinant SUMO E1 ligase purchased from BIOMOL International was used instead of HeLa cell lysate.

**Cell Sorting**—Cell sorting was performed using BD FACSAria Cell Sorter (BD Biosciences) according to the manufacturer's instructions.

## RESULTS

**PML Exists as an Acetylated Protein in HeLa Cells Treated with Trichostatin A**—HDAC inhibitors including TSA induce differentiation, growth arrest, and apoptosis of cancer cells. In addition to their effects on histones, HDAC inhibitors increase the acetylation level of several non-histone proteins, such as transcription factors, cytoskeletal proteins, and molecular chaperones, which are important for their effects on cancer cells (18). These observations prompted us to screen new acetylation targets of TSA with an antibody array assay combined with *in vivo* labeling of acetylated proteins with [<sup>14</sup>C]acetate. Seven spots indicating possible targets of TSA-induced acetylation were detected (supplemental Fig. S1 and Fig. 1A). We focused on one of these targets, PML, a multifunctional protein that is involved in apoptosis, tumor suppression, and cell cycle regulation (2). We set out to confirm whether PML was acetylated *in vivo*. The same anti-PML antibody as used in the antibody array assay immunoprecipitated an ~79-kDa acetylated protein from lysates of TSA-treated HeLa cells (Fig. 1B), suggesting that PML existed as an acetylated protein in them. Of note, the antibody we used detected only a single band of PML, although PML has seven isoforms. The antibody was confirmed to be able to detect all PML isoforms, suggesting that this PML was the main one expressed in HeLa cells (supplemental Fig. S1).

**PML Is Acetylated by p300 and GCN5 in Vitro**—To test whether known histone acetyltransferases (HATs), p300 and GSN5, can acetylate PML, we performed an *in vitro* acetylation assay using GST-PML as a substrate. Both HATs acetylated PML *in vitro* (Fig. 2A), and we focused on the acetylation by p300 that occurred with higher efficiency. Use of a series of PML subdomains in the *in vitro* p300 acetylation assay indicated that PML would be acetylated on the C-terminal domain, amino acids 448–560 (supplemental Fig. S2). Inspection of the

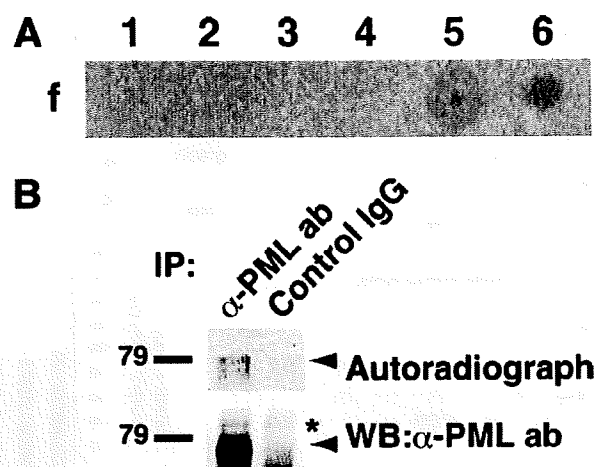


**FIGURE 1. PML exists as an acetylated protein in HeLa cells treated with TSA.** *A*, screening for acetylation targets of TSA by antibody array. Lysate from HeLa cells pulse-labeled with [<sup>14</sup>C]acetate and treated with TSA was incubated with a nitrocellulose array comprising 113 antibodies. After extensive washes, the array was subjected to autoradiography. Similar results were obtained from duplicated experiments. Representative spots are shown. The antibodies used for *f-1* to *f-6* are anti-MEK1/2 antibody, anti-phospho-MEK1/2 antibody, anti-MKP-1 (V-15) antibody, anti-PML (PG-M) antibody, anti-PML (H-238) antibody, and anti-acetylated lysine antibody, respectively. *B*, PML exists as an acetylated protein in TSA-treated HeLa cells. Pulse-labeled HeLa cells with TSA treatment were lysed as in *A*. The lysates were immunoprecipitated (IP) with PML antibody (*ab*) or control rabbit IgG. 90% of the immunoprecipitates were subjected to SDS-PAGE, autoradiography, and detection with phosphorimaging (*upper panel*). 10% of the immunoprecipitates were subjected to SDS-PAGE and immunoblotting with PML antibody (*lower panel*). The positions of PML and nonspecific band are indicated by an arrow and an asterisk, respectively. *WB*, Western blotting.

PML sequence in this region revealed the presence of 7 lysine residues (supplemental Fig. S2); therefore, we introduced a series of arginine substitutions to map the acetylation sites. Within the C-terminal domain of PML, only the substitution of arginine for lysine 487 (K487R) measurably reduced acetylation of PML by p300 among all the individual substitutions (Fig. 2B; mutations are designated by the codon number between Lys and Arg). When arginine substitutions for other lysines were combined with K487R, a further reduction of acetylation was observed with K515R (Fig. 2C). Acetylation of full-length PML was impaired by substitutions of K487R and K487R/K515R similarly to that of the C-terminal domain of PML (Fig. 2D). Our results indicate that the principal sites of p300 acetylation in PML will be lysines 487 and 515.

**PML Acetylation Is Increased in Response to TSA Treatment**—We examined whether PML acetylation by p300 occurred *in vivo* at the same sites as identified *in vitro*. Wild-type PML and PML with the K487R/K515R mutations were designated as PML W and PML M, respectively. Coexpression of p300 enhanced PML W acetylation, whereas acetylation PML M was weak in the basal state and showed no significant response to p300 coexpression (Fig. 3A, *top panel*). The efficiency of immunoprecipitation was the same for all samples (Fig. 3A, *middle panel*), and the increase in acetylation of a 17-kDa protein by coexpression of p300, which suggested the induction of histone acetylation, was equal between transfectants with PML W and PML M (Fig. 3A, *bottom panel*). These results suggest that p300 acetylates PML *in vivo* at the same sites as identified *in vitro*.